- Article type: research paper
- Date text written: 14 November 2013.
- Number of words: 8249, number of figures: 20.

Static Mechanical Properties of Polyvinyl Alcohol Fibre Reinforced Concrete (PVA-FRC)

Author 1

- Amin Noushini, Postgraduate research candidate
- Centre for Built Infrastructure Research (CBIR), University of Technology Sydney, Australia

Author 2

- Kirk Vessalas, Doctor of Civil Engineering
- Centre for Built Infrastructure Research (CBIR), University of Technology Sydney, Australia

Author 3

- Bijan Samali, Professor of Structural Engineering
- Centre for Built Infrastructure Research (CBIR), University of Technology Sydney, Australia

Corresponding author: Amin Noushini
School of Civil and Environmental Engineering
University of Technology Sydney
PO BOX 123, Broadway NSW 2007, Australia
E-mail: amin.noushini@uts.edu.au
Tel: +61 2 9514 9059
Fax: +61 2 9514 2510
Mob: +61 450 805 031

Abstract

This investigation assesses the performance of polyvinyl alcohol (PVA) fibres of two geometric lengths (6 and 12 mm) in concrete. Based on total concrete volume, 4 fibre fractions of 0.125%, 0.25%, 0.375% and 0.50% were evaluated for their effect on fresh and hardened properties of PVA fibre reinforced concretes (PVA-FRCs). Fly ash was also used as partial replacement of Portland cement in all mixes. By carrying out a comprehensive set of experiments, i. e., compressive strength, splitting tensile strength, modulus of elasticity, modulus of rupture and residual flexural strength, it was observed that PVA fibre significantly enhances the static mechanical properties of concrete as well as improving its post peak response and ductile behaviour.

Keywords

Concrete technology & manufacture; Concrete structures; Composite structures.

1. Introduction and Background

Concrete is known to be a brittle like material that has high compressive strength and low tensile strength and strain capacity. No post peak behaviour is demonstrated by concrete. In fact, deteriorations and catastrophic failures that occur without noticeable warning in a concrete structure are due to the brittle nature of this material (Hamoush et al., 2010).

An approach introduced to improve the post peak behaviour and ductile performance of concrete is by using fibres as intrinsic reinforcement (Tadepalli et al., 2013, Daneti et al., 2011). Use of randomly distributed short fibres to improve the physical properties of concrete or other brittle materials is a historical aspect. Straw reinforced mud bricks were used in the Middle East as long as 10,000 years ago. In 1400 BC, sun-baked bricks reinforced with straw were used to build the 57 m high hill of Aqar Quf near Baghdad (Hannant, 2003). Sundried adobe bricks (a mixture of sand, clay and straw) were also used for several centuries in the Americas by the indigenous inhabitants, particularly in the American Southwest and in parts of South America (Mindess, 2007).

The modern usage of fibres in the construction industry goes back about a century (1900s) to the creation of asbestos cement. However, the first theoretical studies of fibre use in concrete were developed in the early 1960s by Romualdi, Batson, and Mandel when these authors published their research (Romualdi and Batson, 1963, Romualdi and Mandel, 1964, Zollo, 1997). The introduction of this research brought fibre reinforced concrete (FRC) to the attention of academic and industry research scientists around the world as a viable solution for improving the post peak behaviour and ductility of concrete. Advancement of FRC research then continued in the 1970s when mostly the integration of glass and steel fibres into concrete were investigated (Perumalsamy and Surendra, 1992). In the middle 1980s, many new fibre types and geometries were introduced, which significantly altered the manufacturing techniques of FRC which in turn influenced the strength and toughness (crack control) of FRCs (Zollo, 1997).

In accordance with the terminology used by the American Concrete Institute (ACI) Committee 544, Fibre Reinforced Concrete, there are four categories of FRC available based on fibre material type. These are SFRC, for steel fibre FRC; GFRC, for glass fibre FRC; SNFRC, for synthetic fibre FRC including carbon fibres; and, NFRC, for natural fibre FRC.

The pioneering work by researchers (Zensveld, 1975, Hannant, 1980, Krenchel and Shah, 1986) on synthetic FRC and cementitious composites, emphasized the need to overcome disadvantages due to the low modulus of elasticity and poor bonding properties of synthetic fibres within the cementitious matrix. The latter is particularly an issue due to the chemical composition and surface properties of synthetic fibres (Bentur and Mindess, 2007).

From amongst the many types of synthetic fibres used in SNFRCs and cementitious composites, polyvinyl alcohol (PVA) fibre is a relatively new inclusion. Polyvinyl alcohol is adopted from polyvinyl acetate, which is readily hydrolysed by treating an alcoholic solution with aqueous acid or alkali (Feldman, 1989), leading to the formation of the structure shown in Figure 1. PVA contains hydroxyl groups (OH), which have the potential to form hydrogen bonds between molecules resulting in a significant change in surface bond strength between PVA fibres and the cementitious matrix (Xu et al., 2010). PVA in the form of a powder has a specific gravity ranging from 1.2 – 1.3 (1200-1300 kg/m^3) (Toutanji et al.). During manufacturing, this powder is heated and extruded to give PVA fibres.

PVA fibre is known to be stable and durable in the alkali environment present in the cementitious matrix (Garcia et al. 1997). These fibres are characterised by their high tensile strength (0.8 – 1.6 GPa), high modulus of elasticity (23 – 40 GPa), high chemical resistance to Portland cement, high affinity to water and no adverse health risks (Redon et al., 2004). The hydrophilic surface of PVA fibres creates a strong chemical bond with the cementitious material. Since PVA fibres are mostly stiffer than the concrete matrix and also provide a strong interfacial bond with the cement matrix, they generally have a positive effect on enhancing the bending strength and other mechanical properties of FRCs (Ogawa and Hoshiro, 2011). The high tensile strength of PVA fibres contributes to sustaining the first crack stress and resisting pull out force due to the strong bond present between the fibre and the cementitious matrix. In contrast, the low lateral resistance of the fibres may also lead to premature fibre rupture before being pulled out of the cementitious matrix (Ogawa and Hoshiro, 2011). PVA fibres elongate and transfer the load to different parts of the cementitious matrix and, as a result, the load applied is distributed more evenly between the loading surfaces.

Although a considerable amount of research has been carried out so far on the concept of using PVA fibre in mortar or other cementitious composites, limited studies have been carried out on the structural properties of PVA fibre reinforced concrete (PVA-FRC). Most previous research on PVA fibre has focused on the effect of this fibre on different characteristics of engineered cementitious composites (ECCs) such as: material properties (Kong et al., 2003, Li and Wang, 2006), structural performance under cyclic loading (Fischer and Li, 2007), nanoscale chemical and microstructural mechanical properties (Sakulich and Li, 2011, Li and Wang, 2006, Li and Stang, 1997), fatigue performance (Zhang and Li, 2002), durability (Şahmaran and Li, 2009, Şahmaran and Li, 2007, Şahmaran and Li, 2008), water permeability (Lepech and Li, 2009), autogenous and drying shrinkage (Şahmaran et al., 2009), cyclic freeze–thaw resistance (Şahmaran et al., 2012) and impact resistance (Yang and Li, 2012).

ECC is a mortar based composite reinforced with short random fibres, to give high ductility. Unlike conventional concrete, ECC has a tensile strain capacity in the range of 3 - 7 %, which is several hundred times more than that of the tensile strain capacity of concrete. The matrix component of ECC is very similar to normal concrete, except ECC does not contain coarse aggregates (Li, 2003).

The isotropic mechanical properties of PVA-ECC give high ductility, high energy absorption capacity (toughness) and high tensile and flexural strength leading to a significant improvement in structural response. Li (Li, 1998) suggests that PVA-ECC has the potential to be used in applications such as seismic retrofits, joints, structures subjected to dynamic and impact loads (e.g. pavements, bridge decks) and concrete covers for durability.

This current study therefore aims to strengthen the gap in knowledge of using PVA fibres in conventional concrete. The main objective of this study is to investigate how the fresh and hardened (mechanical) properties of concrete are affected by addition of a certain amount of PVA fibres. Accordingly, PVA fibres of two geometric lengths (6 and 12 mm) were selected to be investigated in order to evaluate their effect on the fresh and hardened properties of concrete.

2. Experimental program

2.1. *Materials*

Shrinkage limited Portland cement (SLPC) and fly ash (FA) were used as the binder for the FRC mixes. SLPC, complying with Australian Standard AS 3972, Type SL (Table 1), was used in this study to minimise drying shrinkage. The FA used in this study is a low-calcium type with a loss of ignition (LOI) value of 1.65%. The fineness of FA by 45 μm sieve was determined to be 94% passing (tested in accordance with Australian Standard AS 3583.1-1998). The oxide compositions of the binders are listed in Table 2.

From literature (Malhotra, 1990, Meyer, 2009, Siddique, 2004), it has been demonstrated that FA addition to a concrete mix increases long term strength (> 28 days) and durability of the concrete by prolonging the hydration process. The two main products of cement hydration are calcium silicate hydrate (C–S–H) and calcium hydroxide (CH). From these two hydration products, C–S–H is the strengthening phase for concrete where CH has no contribution to strength development (in the absence of supplementary cementitious materials, SCMs). CH is also a potential site of weakness for certain forms of chemical degradation and leads to efflorescence and poor chemical resistance (Neville, 1991). Since FA is a pozzolanic material possessing an aluminosilicate structure, it can react with CH to form additional C–S–H binder, which is deposited in pore spaces. This leads to a gradual densification of the cementitious matrix, which contributes to increased strength, reduced permeability and increased long term durability (Fraay et al., 1989). It has also been reported that FA improves the rheological properties and workability of concrete due to its spherical shaped particles and fineness (Neville, 1991).

Table 1. Typical properties of shrinkage limited cement in accordance with AS 3972 requirements

Property		AS 3972 requirements	Typical properties of project cement
Setting time	(min.)	45 min	1.5 – 3 h
	(max.)	10 h	2.5 – 4 h
Soundness	(max.)	5%	<3%
Drying shrinkage	28-day (max.)	750 µstrain	550 µstrain
Compressive strength	7-day (min.)	35 MPa	42 – 50 MPa
	28-day (min.)	45 MPa	57 – 64 MPa

Table 2. Chemical properties of PC and FA by x-ray fluorescence method

	SiO_2	Al_2O_3	Fe_2O_3	CaO	MgO	Na_2O	K_2O	TiO_2	MnO	P_2O_5	SO_3	LOI
PC [wt. %]	20.16	4.62	4.56	65.35	1.06	-	0.44	0.28	0.60	0.07	2.55	1.16
FA [wt. %]	65.13	23.75	3.38	1.92	0.49	0.48	1.46	0.92	0.07	0.25	0.07	1.65

A maximum nominal size of 20 mm aggregate was used in all mixes. All aggregates used in mix design were sourced from Dunmore, Australia, which includes 50/50 blended fine/coarse manufactured sand and 10 mm and 20 mm crushed latite gravel. The grading of all aggregates as shown in Table 3 were found to comply with the Australian Standard AS 2758.1 specifications and limits.

Table 3. Sieve analysis

Sieve aperture	Fine aggregate		Coarse aggregate			
			10 mm (nominal size)		20 mm (nominal size)	
	Limits[1] [%]	Passing [%]	Limits [%]	Passing [%]	Limits [%]	Passing [%]
26.5 mm	-	-	-	-	100	100
19.0 mm	-	-	-	-	85 to 100	95
13.2 mm	-	-	100	100	-	51
9.5 mm	100	100	85 to 100	87	0 to 20	14
6.7 mm	-	100	-	49	-	6
4.75 mm	90 to 100	98	0 to 20	11	0 to 5	4
2.36 mm	60 to 100	81	0 to 5	3	-	3
1.18 mm	30 to 100	65	0 to 2	2	0 to 2	2
600 µm	15 to 80	55	-	-	-	-
300 µm	5 to 40	38	-	-	-	-
150 µm	0 to 25	8	-	-	-	-
75 µm	0 to 20	4	-	-	-	-
Absorption [%]		1.2%		1.8%		1.6%

[1] Limits define in accordance with AS 2785.1(1998)

Drinkable grade tap water was used for all mixes after conditioning to room temperature (23 ± 2 °C). Furthermore, in order to improve the workability, a polycarboxylic-ether based high range water reducing admixture (HWR), Glenium HWR, was used. Glenium HWR is an innovative admixture based on a modified polycarboxylic ether (PCE) polymer. It greatly enhances the rheological properties of concrete by initiating an electrostatic dispersion mechanism, which stabilises cement particles and their ability to separate and disperse due to electrical repulsion. The typical properties of Glenium HWR are tabulated in Table 4.

Table 4. Typical properties of Glenium 51

Appearance	Brown liquid
Specific Gravity at 20°C	1.095 ± 0.02 g/cm^3
pH value	7.0 ± 1
Alkali content [%]	Less than or equal to 5.0
Chloride content [%]	Less than or equal to 0.10

Uncoated monofilament polyvinyl alcohol fibres of 2 different geometric lengths, 6 and 12 mm, with properties mentioned in

Table 5 and as shown in Figure 2, were used in the PVA-FRC mixes. Both 6 mm ($L_f = 6$ mm) and 12 mm ($L_f = 12$ mm) fibres were determined to have the same diameter ($d_f = 0.014$ mm), thus, the aspect ratio (L_f/d_f) of the longer fibre was twice as large as that of the shorter type (aspect ratio of 857 compared to aspect ratio of 428).

Table 5. Properties of PVA fibres

Type	Density	Length (L_f)	Diameter (d_f)	Tensile strength	Young's Modulus (E_f)	Elongation
	[g/cm^3]	[mm]	[mm]	[MPa]	[GPa]	[%]
PVA-6	1.29	6	0.014	1500	41.7	7
PVA-12	1.29	12	0.014	1500	41.7	7

2.2. Mix proportions and mixing procedure

Mix designs were selected to achieve a characteristic compressive strength (f_c') of 60 MPa. This relatively high strength is selected to ensure that after fibre addition, which may cause strength reduction, the concrete compressive strength still remains in the range of structural concrete (20 MPa to 100 MPa), in accordance with AS 3600 requirements. In order to obtain a desired slump of 80 ± 20 mm, HWR dosage was varied. Mix designations are listed in Table 6 and the details of the mix proportions for all mixes are listed in Table 7.

Table 6. Mix designations

Mix reference	V_f [1] [%]	L_f [mm]	L_f / d_f [2]
Control	-	-	-
6-PVA-0.125	0.125	6	428
6-PVA-0.250	0.250	6	428
6-PVA-0.375	0.375	6	428
6-PVA-0.500	0.500	6	428
12-PVA-0.125	0.125	12	857
12-PVA-0.250	0.250	12	857
12-PVA-0.375	0.375	12	857
12-PVA-0.500	0.500	12	857

[1] fibre volume fraction
[2] fibre aspect ratio

Table 7: Mix proportions

Mix Reference	kg/m^3								Lit/m^3
	SLPC	FA	Sand	Coarse Aggregate		Water [1]	PVA fibre		HWR
				10mm	20mm		6mm	12mm	
Control	301	129	635	390	700	151	0	0	1.215
6-PVA-0.125	301	129	635	390	700	151	1.613	0	1.876
6-PVA-0.250	301	129	635	390	700	151	3.225	0	1.774
6-PVA-0.375	301	129	635	390	700	151	4.838	0	2.143
6-PVA-0.500	301	129	635	390	700	151	6.450	0	2.143
12-PVA-0.125	301	129	635	390	700	151	0	1.613	2.338
12-PVA-0.250	301	129	635	390	700	151	0	3.225	2.468
12-PVA-0.375	301	129	635	390	700	151	0	4.838	2.597
12-PVA-0.500	301	129	635	390	700	151	0	6.450	3.506

[1] w/c (water /cementitious materials) ratio maintained at a constant rate of 0.35 for all mixes.

Mix proportioning of the raw material ingredients was carried out by mass. The fibre volume fractions employed were limited to 0.5%; this limit was derived from the results of several preliminary trial mixes, which indicated that the incorporation of higher volume fractions beyond 0.5% resulted in a loss of cohesiveness of the concrete.

For the non-FRC (control) mix, mixing was performed in accordance with Australian Standard AS 1012.2 test method requirements. However, for FRC mixes, due to the presence of fibres, the standard mixing regime listed in the Australian Standard AS 1012.2 test method for conventional concrete was modified by increasing the mixing time for the various steps outlined in Section 10 of this standard. This was carried out to ensure uniform dispersion of the fibres in PVA-FRC mixes was achieved. Preliminary trials were carried out in order to find the appropriate mixing time required to disperse the 12 mm fibres of 0.500% dosage properly. It was found that the mixing time needed to be increased from 2 to 3 minutes for each of the 3 consecutive mixing stages prescribed in the Australian Standard AS 1012.2 mixing procedure. Fine aggregates were firstly mixed with PVA fibres in a vertical pan mixer until fibres were observed to disperse uniformly. Coarse aggregates were then added and premixed for 3 minutes. Thereafter, SLPC, FA and water were introduced and mixed for 3 minutes. In order to adjust the slump, HWR was added within the first minute of adding cementitious material. Following 3 minutes of mixing, a rest period of 2 minutes was applied followed by a further 3 minutes of mixing. The rest of the mixing procedure was followed as specified in the Australian Standard AS 1012.2 (1994) test method.

Modification of the standard mixing sequence, in order to achieve a more uniform mix, has also been previously described by other researchers. Manolis et al. (Manolis et al., 1997) suggested that 3 to 5 minutes of mixing time was required after fibre addition to achieve proper fibre dispersion.

Slump was measured to ensure the same degree of workability was achieved for each mix and, thereafter, freshly mixed concrete was placed into moulds and consolidated using an external vibrating table. Moulds were covered with plastic sheets to retain moisture. At 24 h for cylindrical specimens and 48 h for prismatic samples, specimens were demoulded and placed in lime-saturated water at a temperature of 20 ± 2 °C until the testing date following Australian Standard AS 1012.8 procedural requirements.

2.3. *Testing methodology*

For each concrete batch, fresh properties, i.e., slump, compacting factor, air content (AC) and mass per unit volume (MPV) were assessed in compliance with Australian Standard AS 1012.3.1, AS 1012.3.2, AS 1012.4.2 and AS 1012.5 test method requirements, respectively. Moreover, in order to evaluate the mechanical properties of the concrete mixes, compressive strength, indirect (splitting) tensile strength, modulus of rupture (MOR), static chord modulus of elasticity (MOE) and residual flexural strength were also investigated following the Australian Standard testing methods AS 1012.9, AS 1012.10, AS 1012.11 and AS 1012.17 and British Standard European Standard BS EN 14651, respectively, at different curing ages (7, 28 and 56 days).

Uniaxial compressive strength and splitting tensile strength tests were performed on 100 × 200 mm cylindrical specimens in accordance with Australian Standard AS 1012.9 and AS 1012.10 test method criteria, respectively. Cylindrical specimens were tested under a load rate control condition in an 1800 kN universal testing machine with the constant load rate applied equivalent to 20 ± 2 MPa per minute for compressive strength testing and 1.5 ± 0.15 MPa per minute for splitting tensile strength testing.

Strain gauges were also attached to certain concrete cylinders to monitor the longitudinal deformation of test specimens under compressive load to failure (see Figure 3).

Flexural tensile strength or MOR was obtained from four-point loading tests carried out on 100 × 100 × 400 mm prisms using a loading rate of 1 ± 0.1 MPa/min until fracture occurred following AS 1012.11 test method requirements. Four-point loading was applied and mid-span deflection of the flexural specimens was measured by means of a linear variable differential transformer (LVDT) that was placed at the centre of each specimen.

Residual flexural tensile strength testing (fracture testing) was carried out on notched 150 × 150 × 550 mm prismatic specimens of following the test method requirements of the British Standard European Standard BS EN 14651. After 25 days curing, a notch was cut into the middle of each specimen using a diamond blade saw. This age was selected for notching of the samples following the prescribed testing methodology in the British Standard European Standard BS EN 14651 to allow for the test specimens to be cured for a minimum of 3 days after sawing. The specimens were rotated 90° around their longitudinal axis and then cut through the width at mid-span as shown in Figure 4. The width and depth of the notch was less than 5 mm and approximately 25 mm for each specimen, respectively. The distance h_{sp}, as shown graphically in Figure 4, was in the range of 125 ± 1 mm. Test specimens were then returned to the curing tank for further curing until 28 days, and then removed from the water 3 hours before testing. In order to carry out the residual flexural tensile strength test, a 500 kN universal testing machine, capable of measuring loads to an accuracy of 0.1 kN, with a controlled load rate, was used to give a constant rate of crack mouth opening displacement (CMOD). A clip gauge (extensometer) with an accuracy of 0.01 mm was also used to measure the CMOD. For CMOD values less than 0.1 mm, the load rate was adjusted so that CMOD could increase at a constant rate of 0.05 mm/min. When CMOD = 0.1 mm, the machine was adjusted to increase CMOD at a constant rate of 0.3 mm/min. The values of load and corresponding CMOD were recorded at a rate of 5 Hz during each test.

The static chord modulus of elasticity (MOE) test was also carried out on 150 × 300 mm cylinders following the stipulated test method criteria listed in Australian Standard AS 1012.17.

3. Results and discussion

3.1. *Fresh properties*

Slump, compacting factor, air content and mass per unit volume of different mixes were deduced in order to evaluate the affect of PVA fibre addition on the properties of freshly mixed concrete. Herein, the results of all these tests, as summarized in Table 8, are discussed.

Table 8. Fresh properties of control concrete and FRCs

Mix reference	HWR/C [%]	Slump [1] [mm]	Compacting factor	Air Content [1] [%]	Mass per unit volume [1] [kg/m^3]
Control	0.33	75	0.85	1.0	2450
6-PVA-0.125	0.47	75	0.84	1.2	2430
6-PVA-0.250	0.54	65	0.82	1.4	2410
6-PVA-0.375	0.59	65	0.85	1.2	2370
6-PVA-0.500	0.65	70	0.89	1.4	2340
12-PVA-0.125	0.45	70	0.82	1.4	2420
12-PVA-0.250	0.54	60	0.84	1.2	2390
12-PVA-0.375	0.62	60	0.81	1.0	2370
12-PVA-0.500	0.88	60	0.84	1.4	2300

[1] Slump, Air content and Mass per unit volume have been calculated to the nearest 5 mm, 0.2% and 10 kg/m^3, respectively, in accordance with AS1012.3.1, AS1012.4.2 and AS1012.5 test method reporting criteria.

When comparing the slump of FRCs to the slump of control concrete (devoid of PVA fibres), increasing fibre addition was observed to result in a drier mix requiring more HWR. In the case of control concrete, introducing 0.33% HWR resulted in the target slump (80 ± 20 mm). However, higher amounts of HWR were needed to be added to FRCs with increasing addition of PVA fibers to achieve the target slump. For most FRCs, even those containing a higher dosage of HWR, lower slump was recorded compared to the control concrete. Furthermore, 12 mm fibre with a larger aspect ratio than the 6 mm fibres shows higher amounts of HWR required for the same fibre volume fraction to achieve approximately the same value of slump. This observation has been reported by other researchers (Hamoush et al., 2010, Hannant et al., 1978, Swamy, 1974, Han et al., 2009), whereby increasing the fibre volume fraction and aspect ratio were found to decrease the workability of concrete incorporating fibres.

Compacting factor, another measure of workability used to describe the consistency of a concrete mix, shows that additions of PVA fibres are almost insignificant in contributing to the concrete self-compacting characteristics, although a small decrease in the compaction factor was recorded for some FRCs compared to the control concrete.

Comparing the AC of FRCs to control concrete versus HWR/C illustrates that the AC of FRCs is slightly higher than that of control concrete, although this improvement is very small in magnitude (see Figure 5). Such observations have been previously reported in literature (Heo et al., 2012) whereby adding fibres to the mix and also increasing the amount of HWR caused a higher air content to result.

The MPV of concrete is observed to decrease with increasing fibre addition in mixes. This decrease in MPV may possibly be due to the lower relative density of the PVA fibres. By increasing the amount of fibre in the mix, it was found that the MPV decreased from 2450 kg/m^3 for the control concrete to 2300 kg/m^3 for the 12-PVA-0.500 mix. This noted decrease in the MPV is highly dependent on the volume and amount of fibres in the cementitious matrix as well as the length and number of fibres. It can also be noted that in the same fibre volume fraction, the 12 mm fibres affect the MPV more so than the 6 mm fibres, which may be attributed to the higher aspect ratio of the longer fibres. This observation has been reported by other researchers (Yap et al., 2013), whereby longer length fibres of same type (i.e. polypropylene fibres) and same specific gravity (0.9) decrease the concrete MPV more so than shorter length fibre for the same fibre volume fraction.

3.2. Mechanical properties

3.2.1. *Compressive strength*

The compressive strength of control concrete and FRCs cylindrical specimens with different fibre volume fractions ranging from 0.0% to 0.5% after 7, 28 and 56 days of age are presented in Table 9 and Figure 6. Standard deviation calculated for compressive strengths of each concrete set, show the level of variation from the average strength reported for 3 specimens tested for each curing age. A lower standard deviation indicates that the individual compressive strength of test specimens tend to be closer to the average strength of that set, which is associated with a higher level of confidence in the statistical average strength reported.

Table 9. Compressive strength of control concrete and FRCs after 7, 28 and 56 days

Mix reference	7 day strength - $f_{c,7}$		28 day strength - $f_{c,28}$		56 day strength - $f_{c,56}$	
	Average Strength [1] [MPa ± SD [2]]	Strength effectiveness [%]	Average Strength [MPa ± SD]	Strength effectiveness [%]	Average Strength [MPa ± SD]	Strength effectiveness [%]
Control	46.0 ± 1.7	N/A	60.0 ± 3.2	N/A	72.5 ± 3.0	N/A
6-PVA-0.125	45.0 ± 0.5	-2.1	65.0 ± 4.6	+8.3	79.0 ± 2.1	+9.0
6-PVA-0.250	48.0 ± 4.1	+4.3	67.0 ± 3.2	+11.7	82.5 ± 4.2	+13.8
6-PVA-0.375	43.0 ± 1.8	-6.5	62.0 ± 2.3	+3.3	73.5 ± 2.6	+1.4
6-PVA-0.500	40.5 ± 3.5	-12.0	61.5 ± 2.5	+2.5	70.0 ± 3.8	-3.4
12-PVA-0.125	41.5 ± 1.0	-9.7	63.0 ± 1.8	+5.0	70.5 ± 2.8	-2.8
12-PVA-0.250	43.5 ± 3.6	-5.4	64.5 ± 3.2	+7.5	73.0 ± 2.9	+0.7
12-PVA-0.375	41.0 ± 2.6	-10.9	60.0 ± 1.7	0.00	67.5 ± 1.5	-6.9
12-PVA-0.500	39.5 ± 2.4	-14.1	58.5 ± 2.8	-2.5	64.0 ± 4.2	-11.7

[1] Average compressive strength of the test specimens calculated to the nearest 0.5 MPa in accordance with AS 1012.9
[2] SD: Standard deviation (reported out of 3 specimens tested for each age)

Strength effectiveness (S.E), which can be defined as the percent increase or decrease in the strength of FRCs compared to the strength of the control concrete at the same curing age has been also calculated.

$$S.E = \frac{FRC\ strength - Control\ concrete\ \ strength}{Control\ concrete\ strength} \times 100\% \qquad (1)$$

The compressive strength values of FRCs after 7, 28 and 56 days have been normalised with respect to the compressive strength of the control concrete at the same curing age and plotted against fibre volume fraction in Figure 7 to Figure 9. In comparison to literature findings (Li, 1992), the compressive strength results indicate that fibres are not beneficial to compressive strength when the fibre content increases beyond a certain amount. As previously found by Li (Li, 1992), the compressive strength may first increase, then decrease, with increasing fibre volume fraction. From this past study, results indicated that two opposing processes of strength improvement and degradation were observed when fibres were added to a cement composite. When fibres are present in the cementitious matrix, strength improvement can possibly be an indication of an increase in the resistance to microcrack sliding and extension, whereas strength degradation can be the resultant of an increase in either pore volume or microcrack density. The pores may have arisen from insufficient consolidation of the fresh concrete and the additional microcracks may have arisen from the contact of fibres, (unbonded) fibre end cracks, poor fibre/matrix bonding or poor adhesion between the filaments within fibre bundles (Li, 1992).

By viewing the results in Figure 6, it can be noted that with the same fibre volume fraction, shorter fibres are observed to enhance compressive strength more so than longer fibres. This observation can be possibly explained by considering the fact that the incorporation of longer length fibres into the mix, make vibration and consolidation more difficult (D. V. Soulioti, 2011), and, thus, this will result in a more porous structure. Since the mechanical properties of a material is mainly governed by its microstructural features like porosity and pore size distribution (Mydin and Soleimanzadeh, 2012), incorporating longer length fibres, which increase the possibility of pores connections in the matrix, leads to a lower strength of the composite. Similar observations for other types of synthetic fibres (i. e., polypropylene fibres) have previously been reported by other researchers (D. V. Soulioti, 2011, Mydin and Soleimanzadeh, 2012). Furthermore, the optimum fibre volume fraction was found to be 0.25% across all curing ages with a 14% increase in compressive strength noted compared to the control concrete after 56 days curing.

Figure 10 shows the compressive strength of all concretes versus curing age. The slopes of the curves in each region (0 – 7 days, 7 – 28 days and 28 – 56 days) demonstrate the rate of strength gain within that period. The slope of the curve between 7 and 28 days for all FRCs is considerably higher than that of the control concrete. This observation possibly suggests that both 6 and 12 mm fibres assist with compressive strength development within this time frame. In other words, the lower 7 day and higher 28 day compressive strengths of FRCs compared to the control concrete indicate that

PVA fibres affect strength gain by decreasing the strength at early ages (after 7 days) and increasing the strength gain from 7 to 28 days. For instance, the PVA-FRC including 0.25% of 6 mm fibres can be seen to achieve the 28 day strength of control concrete at approximately 20 days. This noted increase in strength is most likely due to the enhanced bond strength achieved between the cementitious material and fibres as a function of increasing age.

The slope of the third part of the curve from 28 to 56 days illustrates that 6 mm fibres in low percentages (< 0.25%) contribute to the strength gain of concrete from 28 to 56 days; however, higher additions of 6 mm fibre and all additions of 12 mm fibre affect the strength gain in this period with lower strength gain achieved compared to the control concrete after 56 days curing. Here again the PVA-FRC having 0.25% of 6 mm fibres can be seen to reach the 56 day strength of control concrete at 38 days of age.

If the 56 day strength of control concrete and FRCs are assumed to be their ultimate strength, then the ratio of compressive strength after 7 and 28 days to the ultimate strength, which is called ‘relative strength’, can be calculated using Equation (2). These values are presented in Table 10.

$$\textit{Relative strength}_{x\text{-}56} = \frac{f_{c,x}}{f_{c,56}} \times 100\% \qquad (2)$$

where x is the specific curing age which can be either 7 or 28 days.

Table 10. Relative compressive strengths for control concrete and FRCs

Mix reference	Relative strength$_{7\text{-}56}$ [%]	Relative strength$_{28\text{-}56}$ [%]
Control	63.4	82.8
6-PVA-0.125	57.0	82.3
6-PVA-0.250	58.2	81.2
6-PVA-0.375	58.5	84.3
6-PVA-0.500	57.9	87.9
12-PVA-0.125	58.9	89.4
12-PVA-0.250	59.6	88.4
12-PVA-0.375	60.7	88.9
12-PVA-0.500	61.7	91.4

Qualitative observations carried out during the compressive strength test indicate that the failure modes for FRCs and control concrete are significantly different. For control concrete, failure was seen to be quite brittle with the specimens failing in an almost explosive-like manner. Control concrete specimens at later curing ages failed with a more pronounced explosive-like failure compared to that of early ages. Whereas, for FRCs, more ductile behaviour was observed during failure and depending on the fibre volume fraction, specimens were noted to destruct with the presence of many cracks on the surface.

The integrity of FRC specimens was found to improve due to the restriction of PVA fibres. From previous research (Meda et al., 2012), it has been stated that the presence of fibres in concrete assist by avoiding a sudden and brittle like failure due to their ability to enhance concrete toughness in compression. For FRC specimens of higher fibre additions, i.e., 0.50%, an unloading process was observed once the load reached the critical stress value and the failure mode thereafter was seen to be almost ductile. Consequently, the incorporation of fibres greatly improves the compressive failure mode of concrete specimens, which has been also previously reported by Zheng et al. (Zheng et al., 2012). It has been also reported (Lam et al., 1998) that by using FA in concrete, the post peak compressive behaviour of concrete will increase and the strain value at maximum stress will improve.

Previous research (De Nicolo et al., 1994) has indicated that the strain at peak stress in uniaxial compression for conventional concrete after 28 days curing is typically 0.002. However, mix composition, curing conditions, shape and size of specimen, loading rate, age of loading, and test techniques used, all have a bearing on this resulting strain (Tasdemir et al., 1998). Herein, the strain corresponding to ultimate stress of FRCs are given in Table 11.

It has been previously reported by Tasdemir et al. (Tasdemir et al., 1998) that the strain at peak load decreases as the compressive strength of concrete decreases. However, from the results shown in Table 11 in this study, it can be seen that for FRCs, strain at peak stress increases although the compressive strength decreases. This noted increase in strain possibly may be due to the presence of fibres in the matrix contributing to filling the voids in the interfacial transition zone (ITZ) between the matrix and aggregates in concrete and making these regions more structured (Palmquist et al., 2011). Past studies (Tasdemir et al., 1998) have demonstrated that the ITZ plays an important role in the resultant shape of the stress-strain curve under uniaxial compression.

Table 11. Stress and strain at ultimate stress in compression after 28 days for FRCs versus control concrete

Mix Reference	V_f [%]	$f_{c,28}$ [MPa]	Strain at peak stress (ε_{cu})
Control	0.00	57.5	0.0025
6-PVA-0.125	0.125	65.0	0.0025
6-PVA-0.250	0.250	67.0	0.0026
6-PVA-0.375	0.375	62.0	0.0030
6-PVA-0.500	0.500	61.5	0.0034
12-PVA-0.125	0.125	63.0	0.0026
12-PVA-0.250	0.250	64.5	0.0026
12-PVA-0.375	0.375	60.0	0.0031
12-PVA-0.500	0.500	58.5	0.0035

3.2.2. *Indirect tensile strength*

The indirect tensile (splitting tensile) strength of control concrete and FRCs with 0.25% and 0.5% fibre volume fractions after 7, 28 and 56 days of age are presented in Table 12. As reported in Table 12, the splitting tensile strength of conventional concrete is significantly enhanced by introducing PVA fibres to the mix. The $f_{ct.sp,28}$ values of all FRCs were found to be higher than that of control concrete, ranging from 11% for 12-PVA-0.500 to 32.5% for 6-PVA-0.250. Figure 11 shows the normalised indirect tensile strength of FRCs after 7, 28 and 56 days with respect to the control concrete. It also worth noting that although the incorporation of higher than 0.25% volume fraction or longer length fibres (12 mm compared to 6 mm) did not lead to a higher splitting tensile strength, which may be due to more porous structure as stated before for the results observed for compressive strength (D. V. Soulioti, 2011, Mydin and Soleimanzadeh, 2012), the presence of fibres enhanced the ductile behaviour of concrete by improving its post-peak behaviour. Previous studies (Padron and Zollo, 1990, Hannant, 2003) reveal that the effect of fibre addition to the concrete is more in line with energy absorption and crack control rather than in increasing the load bearing capacity. Fibres assist with increasing the volumetric strain capacity of concrete after cracking by bridging the cracks and, thereby, improving the post peak behaviour of FRC (Soroushian and Bayasi, 1991, Bayasi and Zeng, 1993, ACI, 1993).

Table 12. Indirect (splitting) tensile strength of control concrete and FRCs after 7, 28 and 56 days

Mix reference	7 day - $f_{ct.sp,7}$		28 day - $f_{ct.sp,28}$		56 day - $f_{ct.sp,56}$	
	Average strength[1] [MPa]	Standard deviation [MPa]	Average strength [MPa]	Standard deviation [MPa]	Average strength [MPa]	Standard deviation [MPa]
Control	3.0	0.3	3.7	0.5	4.3	0.2
6-PVA-0.250	3.9	0.2	4.9	0.2	5.7	0.3
6-PVA-0.500	3.1	0.1	4.2	0.3	4.6	0.1
12-PVA-0.250	4.0	0.3	4.7	0.2	5.5	0.1
12-PVA-0.500	3.0	0.2	4.1	0.4	4.3	0.4

[1] Average splitting tensile strength of the test specimens calculated to the nearest 0.1 MPa in accordance with AS 1012.10

3.2.3. *Modulus of rupture*

The flexural strength or MOR test of control concrete and FRCs with 0.25% and 0.5% fibre volume fractions were carried out after 7, 28 and 56 days of curing and these results are presented in Table 13.

Table 13. Flexural strength of control concrete and FRCs after 7, 28 and 56 days

Mix reference	7 day - $f_{ct.f,7}$		28 day - $f_{ct.f,28}$		56 day - $f_{ct.f,56}$	
	Average strength[1] [MPa]	Standard deviation [MPa]	Average strength [MPa]	Standard deviation [MPa]	Average strength [MPa]	Standard deviation [MPa]
Control	4.4	0.3	5.6	0.2	7.1	0.2
6-PVA-0.250	4.8	0.1	6.8	0.2	8.3	0.4
6-PVA-0.500	4.1	0.2	6.3	0.1	7.2	0.1
12-PVA-0.250	4.7	0.1	6.7	0.2	7.6	0.5
12-PVA-0.500	4.1	0.3	6.2	0.5	6.6	0.1

[1] Average MOR of the test specimens calculated to the nearest 0.1 MPa in accordance with AS 1012.11

Figure 12 shows the normalised modulus of rupture of FRCs after 7, 28 and 56 days with respect to the MOR of control concrete.

Similar to the results displayed for the splitting tensile strength, the results of flexural strength for FRCs after 28 days ($f_{ct.f,28}$) show significant improvement in strength ranging from 11% up to 21.5%. The highest value of flexural strength was found for the 0.25% volume fraction. At this dosage, fibres in the concrete provide a proper bridging effect, which leads to strength improvement; however, higher fibre content has also adverse effects. These adverse effects can be caused by poor fibre distribution and improper orientation due to the large number of fibres present in the mix. Fibres which are not parallel to the cracks, can contribute to the stress bridging process by preventing a proper fibre orientation. Furthermore, as it is inferred from the results in this study, shorter fibres demonstrate improved flexural strength. A higher aspect ratio of the fibres can be also responsible for this effect. It is assumed that these fibres may bend and not remain aligned in the matrix. Therefore, their total length cannot contribute to the load bearing process and stress control mechanism.

Figure 13 illustrates the load-mid span deflection of test specimens in flexure after 28 days of curing. It can be observed that fracture and total failure in the conventional concrete occurred suddenly after exceeding the maximum load with a drop noted in the load-deflection curve. However, the load-deflection curves of FRCs vary significantly. FRCs show larger deflections at the ultimate stress as well as loads beyond ultimate stress when compared to the control concrete. This will result in a larger area under the load-deflection curves, which is an indication of increasing toughness (Low and Beaudoin, 1994, Jastrzebski, 1977). Consequently, it can be stated that the flexural toughness of concrete enhances by introducing PVA fibres to the mix and it is further enhanced if more fibres are added.

The slope of the load-deflection curve in flexure represents the flexural stiffness (Wight and MacGregor, 2011). As observed from Figure 13, the FRCs flexural stiffness is lower than the control concrete although FRCs have higher load bearing capacities. This behaviour which is the likely result of fibre bridging in the concrete matrix may give rise to a few concerns regarding the serviceability state by imposing larger deflections; however, this is proper behaviour for concrete in seismic applications. This kind of behaviour caters for larger deflections before failure and dissipates more energy compared to conventional concrete in a critical situation such as an earthquake.

Figure 14 shows the normalized peak load deflection of FRCs of both fibre lengths. The peak load deflection is noted to improve more than three times when fibres are added to the control concrete. However, for fibre content more than 0.25% no significant improvement in peak load deflection was observed.

3.2.4 *Modulus of elasticity*

Static chord modulus of elasticity (MOE) of FRCs and control concrete after 7, 28 and 56 days curing are compared in Table 14. From the results, it can be noted that MOE of concrete mixes increase with age. It is also evident that PVA fibres used in low volume fractions (< 0.50%) do not significantly affect the MOE of concrete although some fluctuations in the data were observed. These variations are more noticeable at early ages (7 and 28 days) while after 56 days most FRCs have very close values to that of control concrete.

These observations have been also reported by other researchers. In past studies, different types of fibres, with various values of MOE, do not significantly affect the values of static MOE of concretes, due to a low fibre content (Hannant, 2003, Corinaldesi and Moriconi, 2011). However, it is anticipated that within the FRCs, adding more fibres leads to a decrease in MOE and for the same fibre content longer fibres lead to lower MOE of the concrete.

Table 14. Elastic modulus of control concrete and FRCs after 7, 28 and 56 days

Mix reference	$E_{c,7}$ [1] [GPa]	$E_{c,28}$ [GPa]	$E_{c,56}$ [GPa]
Control	37.7	39.3	41.4
6-PVA-0.250	39.0	40.1	41.9
6-PVA-0.500	33.3	38.8	40.0
12-PVA-0.250	35.0	39.2	40.3
12-PVA-0.500	32.1	33.2	38.7

[1] Elastic modulus of the test specimens calculated to the nearest 0.1 GPa in accordance with AS 1012.17

Previous investigations (Siddique, 2004, Bouzoubaâ et al., 2001, Gencel et al., 2012) on conventional concrete show that the MOE of concrete has a direct relationship with compressive strength and an in-direct relationship with AC. The trend noted in MOE, compressive strength and AC follow these previous observations (see Figure 16 to Figure 18).

3.2.5 *Residual flexural tensile strength*

In order to evaluate the concrete post peak properties, the notched beam test using crack mouth opening displacement (CMOD) has proven to be a reliable test to evaluate the post peak behaviour and toughness of fibre reinforced concrete (Gopalaratnam and Gettu, 1995).

Addition of synthetic fibres does not affect the pre peak behaviour (Meddah and Bencheikh, 2009), whereas in the post peak response the reverse is true. The post peak behaviour of concrete and its elastic behaviour has been investigated in past studies and the results suggest that although fibre addition does not greatly increase the flexural strength it generally improves concrete toughness (Buratti et al., 2011). Moreover, synthetic fibres have been reported to improve the post peak response of concrete in aiding to reduce the rate of strength loss from the peak value (Pantazopoulou and Zanganeh, 2001). Other research investigations carried out on long synthetic and steel fibres (e.g. more than 30 mm length) reported that fibres significantly improve the post peak behaviour and residual flexural strength of conventional concrete (Buratti et al., 2011).

From the results of three-point bending tests carried out on notched prisms at the age of 28 days, the load-crack mouth opening displacement (F-CMOD) relationship was established (Figure 19). The test was carried out on the control concrete and FRCs with fibre content of 0.5%.

From these relationships, the load at the limit of proportionality (F_L) of concrete samples can be evaluated. According to the definition stated in the European Standard EN 14651:2005, F_L is equal to the highest value of the load recorded up to a CMOD of 0.05 mm. Thus, concrete limit of proportionality (LOP) can be calculated using the expression given in Equation (3);

$$f_{ct}^{f} L = \frac{3F_L l}{2bh_{sp}^2} \tag{3}$$

where $f_{ct}^{f}L$ is the limit of proportionality (LOP) in MPa, F_L is the load corresponding to the LOP in N, b (150 mm) and l (500 mm) are the width and span length of the specimen, respectively, and h_{sp} (125 mm) is the distance between the tip of the notch and top of the specimen. All these expressions have been defined assuming a linear stress distribution applied to the cross section.

From the analysis of the F-CMOD relationship, F_L and LOP were calculated and the results are presented in Table 4. F_L can be defined as the load corresponding to the first crack and limit of proportionality (LOP) is derived from the stress at the first crack (Giaccio et al., 2008).

Table 15. Limit of proportionality and residual flexural strength of control concrete and FRCs after 28 days

Mix reference	F_L [kN]	LOP [MPa]	F_1 [kN]	$f_{R,1}$ [MPa]
Control	14.5	4.6	2.3	0.7
6PVA-0.50%	15.0	4.8	5.0	1.6
12PVA-0.50%	15.5	5.0	6.0	1.9

From the load-CMOD curve shown in Figure 19, the residual flexural tensile strength, which represents the load carrying capacity at different CMODs (Figure 20) can also be calculated using the expression given in Equation (4);

$$f_{R,j} = \frac{3F_j l}{2bh_{sp}^2} \tag{4}$$

where $f_{R,j}$ is the residual flexural tensile strength corresponding to CMOD = $CMOD_j$ (j = 1, 2, 3 and 4) in MPa and F_j is the load corresponding to $CMOD_j$ in N. The value of different CMODs are defined in Figure 20, which are: $CMOD_1$ = 0.5 mm, $CMOD_2$ = 1.5 mm, $CMOD_3$ = 2.5 mm and $CMOD_4$ = 3.5 mm.

In accordance with the European Standard EN 14651:2005, the residual flexural tensile strength values are calculated by assuming a linear elastic distribution of stresses at the fracture point.

The load-CMOD curves shown in Figure 19 of all concrete mixes indicate that after the peak load, a load decay occurs and the value of F_j corresponding to $CMOD_2$ = 1.5 mm is approximately equal to zero, which gives zero residual flexural tensile strength. The only $f_{R,j}$ calculated is for $CMOD_1$ = 0.5 mm. The results for $f_{R,1}$ of the different concretes are presented in Table 15.

Based on the test results, control concrete and FRCs have approximately the same values for F_L and limit of proportionality. However, in terms of the post-peak behaviour and residual strength, it can be observed that FRCs have significantly higher values. The load and the residual strength corresponding to crack opening of 0.5 mm have increased two-fold by adding PVA fibres to the mix. This observation indicates that PVA fibre addition to the mix can improve the post-peak response of conventional concrete and increase its residual strength.

4. Summary and conclusions

The following conclusions can be drawn from the current results:

a) Less workability is observed for mixes having more PVA fibre content and higher amount of HWR. Mixes with longer PVA fibre length demonstrate lower slump compared to shorter PVA fibre length for the same PVA fibre volume addition. As a result, it can be concluded that by adding hydrophilic PVA fibres the concrete slump decreases.

b) Mass per unit volume of concrete is seen to decrease by adding PVA fibres to the mix (1% – 6% lower MPV is found for FRCs compared to the control concrete).

c) Compressive strength after 28 days ($f_{c,28}$) increases as PVA fibre addition increases and optimum fibre volume fraction is found to be 0.25% with a 12% improvement noted in $f_{c,28}$. It can also be concluded that shorter PVA fibres increase compressive strength more so compared to longer length PVA fibres. The 28 day compressive strength of FRCs made with different volume fractions of 6 mm PVA fibre is found to be 6.5% higher than that of control concrete, where this value is 2.5% higher for FRCs made with 12 mm PVA fibres.

d) PVA-FRCs cater for a more ductile mode of failure compared to control concrete devoid of fibre additions. Strain at ultimate stress behaviour is observed to be higher with higher fibre contents. The strains of FRCs at peak stress (ε_{cu}) ranged between 0.0026 to 0.0035 compared to 0.0025 for control concrete.

e) The same trend as compressive strength is also observed for tensile and flexural strengths. A 20% increase in flexure and 30% in splitting tensile at 0.25% volume fraction shows how PVA fibre can improve the strength of conventional concrete. Furthermore, conventional concrete specimens failed immediately by a single crack, and separation into two pieces. On the contrary, the PVA-FRC specimens, retained post cracking ability to carry further loads.

f) MOE results show that PVA fibres in low volume fractions used in this study (< 0.50%) do not significantly affect MOE of concrete. Some variations are noticed after early ages (7 and 28 days) while after 56 days most FRCs are similar (38.7 – 41.9 GPa) to that of control concrete (41.4 GPa). However, it is anticipated that within the FRCs, adding more PVA fibres will lead to a decrease in the MOE of concrete and for the same fibre content longer PVA fibres will also lower the MOE of concrete.

g) In terms of the post peak behaviour and residual strength, results indicate that FRCs have improved performance and significantly higher values. The load and residual strength corresponding to the crack opening of 0.5 mm have doubled by adding PVA fibres to the concrete. This indicates that PVA fibre addition to the concrete mix can improve the post peak response of conventional concrete and increase its residual strength. It also worth noting that the LOP of PVA-FRCs made with 0.5% of 6 and 12 mm PVA fibres is found to be slightly higher than that of control concrete (4.8 and 5.0 MPa for FRCs compared to 4.6 MPa for control).

Acknowledgements

The support from Centre for Built Infrastructure Research (CBIR) at University of Technology Sydney (UTS) is acknowledged here.

References

ACI, A. C. I.-. 1993. Guide for Specifying, Proportioning, Mixing, Placing, and Finishing Steel Fiber Reinforced Concrete. *ACI 544.3R-93.* Farmington Hills.

BAYASI, Z. & ZENG, J. 1993. Properties of Polypropylene Fiber Reinforced Concrete. *American Concrete Institute,* 90**,** 605-610.

BENTUR, A. & MINDESS, S. 2007. *Fibre Reinforced Cementitious Composites,* Abingdon, England, Taylor & Francis.

BOUZOUBAÂ, N., ZHANG, M. H. & MALHOTRA, V. M. 2001. Mechanical properties and durability of concrete made with high-volume fly ash blended cements using a coarse fly ash. *Cement and Concrete Research,* 31**,** 1393-1402.

BURATTI, N., MAZZOTTI, C. & SAVOIA, M. 2011. Post-cracking behaviour of steel and macro-synthetic fibre-reinforced concretes. *Construction and Building Materials,* 25**,** 2713-2722.

CORINALDESI, V. & MORICONI, G. 2011. Characterization of self-compacting concretes prepared with different fibers and mineral additions. *Cement and Concrete Composites,* 33**,** 596-601.

D. V. SOULIOTI, N. M. B., A. PAIPETIS AND T. E. MATIKAS 2011. Effects of Fibre Geometry and Volume Fraction on the Flexural Behaviour of Steel-Fibre Reinforced Concrete. *Strain,* 47**,** e535–e541.

DANETI, S. B., WEE, T.-H. & THANGAYAH, T. S. O. 2011. Effect of polypropylene fibres on the shrinkage cracking behaviour of lightweight concrete. *Magazine of Concrete Research* [Online], 63. Available: http://www.icevirtuallibrary.com/content/article/10.1680/macr.2011.63.11.871.

DE NICOLO, B., PANI, L. & POZZO, E. 1994. Strain of concrete at peak compressive stress for a wide range of compressive strengths. *Materials and Structures,* 27**,** 206-210.

FELDMAN, D. 1989. *Polymeric Building Materials,* London, Elsevier Applied Science.

FISCHER, G. & LI, V. C. 2007. Effect of fiber reinforcement on the response of structural members. *Engineering Fracture Mechanics,* 74**,** 258-272.

FRAAY, A. L. A., BIJEN, J. M. & DE HAAN, Y. M. 1989. The reaction of fly ash in concrete a critical examination. *Cement and Concrete Research,* 19**,** 235-246.

GENCEL, O., KOKSAL, F., OZEL, C. & BROSTOW, W. 2012. Combined effects of fly ash and waste ferrochromium on properties of concrete. *Construction and Building Materials,* 29**,** 633-640.

GIACCIO, G., TOBES, J. M. & ZERBINO, R. 2008. Use of small beams to obtain design parameters of fibre reinforced concrete. *Cement and Concrete Composites,* 30**,** 297-306.

GOPALARATNAM, V. S. & GETTU, R. 1995. On the characterization of flexural toughness in fiber reinforced concretes. *Cement and Concrete Composites,* 17**,** 239-254.

HAMOUSH, S., ABU-LEBDEH, T. & CUMMINS, T. 2010. Deflection behavior of concrete beams reinforced with PVA micro-fibers. *Construction and Building Materials,* 24**,** 2285-2293.

HAN, C.-G., HAN, M.-C. & HEO, Y.-S. 2009. Improvement of residual compressive strength and spalling resistance of high-strength RC columns subjected to fire. *Construction and Building Materials,* 23**,** 107-116.

HANNANT, D. J. Year. Polymer fibre reinforced cement and concrete. *In:* ROY, D. M., MAJUMDAR, A. J., SHAH, S. P. & MANSON, J. A., eds. Advances in Cement-Matrix Composites, 1980 Materials Research Society, Pittsburgh, PA. 171-180.

HANNANT, D. J. 2003. Fibre-reinforced concrete. *In:* NEWMAN, J. & CHOO, B. S. (eds.) *Advanced Concrete Technology Set.* Oxford: Butterworth-Heinemann.

HANNANT, D. J., ZONSVELD, J. J. & HUGHES, D. C. 1978. Polypropylene film in cement based materials. *Composites,* 9**,** 83-88.

HEO, Y.-S., SANJAYAN, J. G., HAN, C.-G. & HAN, M.-C. 2012. Relationship between inter-aggregate spacing and the optimum fiber length for spalling protection of concrete in fire. *Cement and Concrete Research,* 42**,** 549-557.

JASTRZEBSKI, J. D. 1977. *The Nature and Properties of Engineering Materials,* New York, John Wiley & Sons.

KONG, H.-J., BIKE, S. G. & LI, V. C. 2003. Constitutive rheological control to develop a self-consolidating engineered cementitious composite reinforced with hydrophilic poly(vinyl alcohol) fibers. *Cement and Concrete Composites,* 25**,** 333-341.

KRENCHEL, H. & SHAH, S. P. 1986. Synthetic fibre for tough and durable concrete. *In:* SWAMY, R. N., WAGSTAFFE, R. L. & OAKLEY, D. R. (eds.) *Developments in Fibre Reinforced Cement and Concrete.* Sheffield: RILEM Symp.

LAM, L., WONG, Y. L. & POON, C. S. 1998. Effect of Fly Ash and Silica Fume on Compressive and Fracture Behaviors of Concrete. *Cement and Concrete Research,* 28**,** 271-283.

LEPECH, M. D. & LI, V. C. 2009. Water permeability of engineered cementitious composites. *Cement and Concrete Composites,* 31**,** 744-753.

LI, V. C. 1992. A simplified micromechanical model of compressive strength of fiber-reinforced cementitious composites. *Cement and Concrete Composites,* 14**,** 131-141.

LI, V. C. 1998. Engineered Cementitious Composites-Tailored Composites Through Micromechanical Modeling. *In:* BANTHIA, N., BENTUR, A. & MUFTI, A. A. (eds.) *Fiber Reinforced Concrete: Present and the Future.* Montreal: Canadian Society for Civil Engineering.

LI, V. C. 2003. On Engineered Cementitious Composites (ECC); A Review of the Material and Its Applications. *Journal of Advanced Concrete Technology,* 1**,** 215-230.

LI, V. C. & STANG, H. 1997. Interface property characterization and strengthening mechanisms in fiber reinforced cement based composites. *Advanced Cement Based Materials,* 6**,** 1-20.

LI, V. C. & WANG, S. 2006. Microstructure variability and macroscopic composite properties of high performance fiber reinforced cementitious composites. *Probabilistic Engineering Mechanics,* 21**,** 201-206.

LOW, N. M. P. & BEAUDOIN, J. J. 1994. The flexural toughness and ductility of portland cement-based binders reinforced with wollastonite micro-fibres. *Cement and Concrete Research,* 24**,** 250-258.

MALHOTRA, V. M. 1990. Durability of concrete incorporating high-volume of low-calcium (ASTM Class F) fly ash. *Cement and Concrete Composites,* 12**,** 271-277.

MANOLIS, G. D., GAREIS, P. J., TSONOS, A. D. & NEAL, J. A. 1997. Dynamic properties of polypropylene fiber-reinforced concrete slabs. *Cement and Concrete Composites,* 19**,** 341-349.

MEDA, A., MINELLI, F. & PLIZZARI, G. A. 2012. Flexural behaviour of RC beams in fibre reinforced concrete. *Composites Part B: Engineering,* 43**,** 2930-2937.

MEDDAH, M. S. & BENCHEIKH, M. 2009. Properties of concrete reinforced with different kinds of industrial waste fibre materials. *Construction and Building Materials,* 23**,** 3196-3205.

MEYER, C. 2009. The greening of the concrete industry. *Cement and Concrete Composites,* 31**,** 601-605.

MINDESS 2007. Thirty years of Fibre Reinforced Concrete research at the UWM British Colombia. *In:* INT, P. (ed.). Sustainable construction materials and technologies.

MYDIN, M. A. O. & SOLEIMANZADEH, S. 2012. Effect of polypropylene fiber content on flexural strength of lightweight foamed concrete at ambient and elevated temperatures. *Advances in Applied Science Research,* 3**,** 2837-2846

NEVILLE, A. 1991. *Properties of Concrete*.

OGAWA, A. & HOSHIRO, H. 2011. Durability of Fibres. *In:* WITTMANN, F. & VAN ZIJL, G. (eds.) *Durability of Strain-Hardening Fibre-Reinforced Cement-Based Composites (SHCC).* Springer Netherlands.

PADRON, I. & ZOLLO, R. F. 1990. Effect of synthetic fibers on volume stability and cracking of Portland cement concrete and mortar. *ACI J.,* 87**,** 327-332.

PALMQUIST, S. M., KINTZEL, E. & ANDREW, K. 2011. Scanning Electron Microscopy to Examine Concrete with Carbon Nanofibers. *5th Pan American Conference for NDT* Cancun, Mexico.

PANTAZOPOULOU, S. J. & ZANGANEH, M. 2001. Triaxial Tests of Fiber-Reinforced Concrete. *Journal of Materials in Civil Engineering,* 13**,** 340-348.

PERUMALSAMY, N. B. & SURENDRA, P. S. 1992. *Fiber-reinforced cement composites,* New York, McGraw-Hill.

REDON, C., LI, V. C., WU, C., HOSHIRO, H., SAITO, T. & OGAWA, A. 2004. Measuring and modifying interface properties of PVA fibers in ECC matrix. *ASCE Journal of Materials in Civil Engineering*.

ROMUALDI & BATSON 1963. Mechanics of crack arrest in Concrete. *ASCE Journal of Engineering Mechanics* 89**,** 147-168.

ROMUALDI & MANDEL 1964. 'Tensile strength of concrete affected by uniformly distributed closely spaced short length of wire reinforcement. *American concrete institute,* 61.

ŞAHMARAN, M., LACHEMI, M., HOSSAIN, K. M. A. & LI, V. C. 2009. Internal curing of engineered cementitious composites for prevention of early age autogenous shrinkage cracking. *Cement and Concrete Research,* 39**,** 893-901.

ŞAHMARAN, M. & LI, V. C. 2007. De-icing salt scaling resistance of mechanically loaded engineered cementitious composites. *Cement and Concrete Research,* 37**,** 1035-1046.

ŞAHMARAN, M. & LI, V. C. 2008. Durability of mechanically loaded engineered cementitious composites under highly alkaline environments. *Cement and Concrete Composites,* 30**,** 72-81.

ŞAHMARAN, M. & LI, V. C. 2009. Durability properties of micro-cracked ECC containing high volumes fly ash. *Cement and Concrete Research,* 39**,** 1033-1043.

ŞAHMARAN, M., ÖZBAY, E., YÜCEL, H. E., LACHEMI, M. & LI, V. C. 2012. Frost resistance and microstructure of Engineered Cementitious Composites: Influence of fly ash and micro poly-vinyl-alcohol fiber. *Cement and Concrete Composites,* 34**,** 156-165.

SAKULICH, A. R. & LI, V. C. 2011. Nanoscale characterization of engineered cementitious composites (ECC). *Cement and Concrete Research,* 41**,** 169-175.

SIDDIQUE, R. 2004. Performance characteristics of high-volume Class F fly ash concrete. *Cement and Concrete Research,* 34**,** 487-493.

SOROUSHIAN, P. & BAYASI, Z. 1991. Fiber Type Effects on the Performance of Steel Fiber Reinforced Concrete *Fiber Type Effects on the Performance of Steel Fiber Reinforced Concrete* 88**,** 359-366.

SWAMY, R. 1974. The technology of steel fibre-reinforced concrete for practical applications. *Proceedings of the Institution of Civil Engineers, London, May 1994,* 56(1)**,** pp.143-159.

TADEPALLI, P. R., MO, Y. L. & HSU, T. T. C. 2013. Mechanical properties of steel fibre concrete. *Magazine of Concrete Research* [Online], 65. Available: http://www.icevirtuallibrary.com/content/article/10.1680/macr.12.00077.

TASDEMIR, M. A., TASDEMIR, C., AKYÜZ, S., JEFFERSON, A. D., LYDON, F. D. & BARR, B. I. G. 1998. Evaluation of strains at peak stresses in concrete: A three-phase composite model approach. *Cement and Concrete Composites,* 20**,** 301-318.

TOUTANJI, H., XU, B., GILBERT, J. & LAVIN, T. Properties of poly(vinyl alcohol) fiber reinforced high-performance organic aggregate cementitious material: Converting brittle to plastic. *Construction and Building Materials,* 24**,** 1-10.

WIGHT, J. K. & MACGREGOR, J. G. 2011. *Reinforced Concrete: Mechanics and Design*, Pearson Education, Limited.

XU, B., TOUTANJI, H. A. & GILBERT, J. 2010. Impact resistance of poly(vinyl alcohol) fiber reinforced high-performance organic aggregate cementitious material. *Cement and Concrete Research,* 40**,** 347-351.

YANG, E.-H. & LI, V. C. 2012. Tailoring engineered cementitious composites for impact resistance. *Cement and Concrete Research,* 42**,** 1066-1071.

YAP, S. P., ALENGARAM, U. J. & JUMAAT, M. Z. 2013. Enhancement of mechanical properties in polypropylene– and nylon–fibre reinforced oil palm shell concrete. *Materials & Design,* 49**,** 1034-1041.

ZENSVELD, J. J. Year. Properties and testing of concrete containing fibres other than steel. *In:* NEVILLE, A., ed. Fibre Reinforced Cement and Concrete, 1975 Lancaster, England. The Construction Press, 217-226.

ZHANG, J. & LI, V. C. 2002. Monotonic and fatigue performance in bending of fiber-reinforced engineered cementitious composite in overlay system. *Cement and Concrete Research,* 32**,** 415-423.

ZHENG, W., LI, H. & WANG, Y. 2012. Compressive behaviour of hybrid fiber-reinforced reactive powder concrete after high temperature. *Materials & Design,* 41**,** 403-409.

ZOLLO, R. F. 1997. Fiber-reinforced concrete: an overview after 30 years of development. *Cement and Concrete Composites,* 19**,** 107-122.

List of Tables

List of Figures

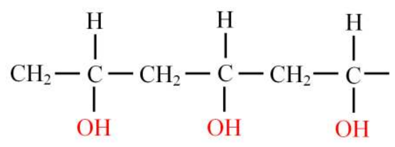

Figure 1. PVA fibre structure

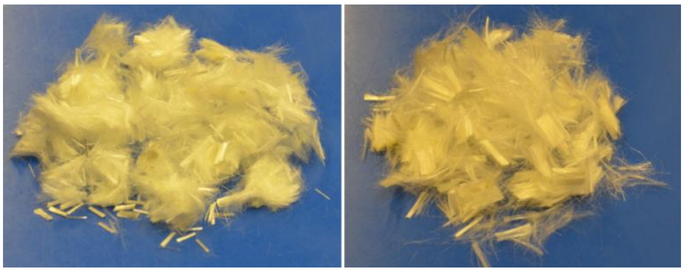

Figure 2: PVA fibres; 6 mm fibres (left) 12 mm fibres (right)

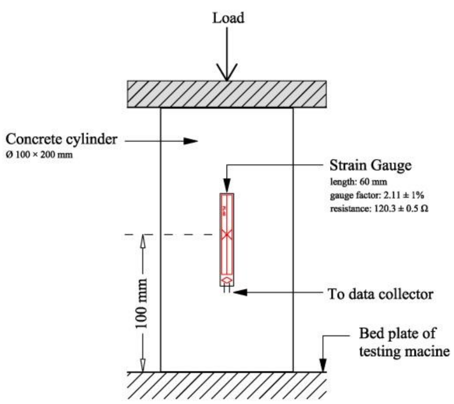

Figure 3. Schematic of compressive strength test with strain gauge

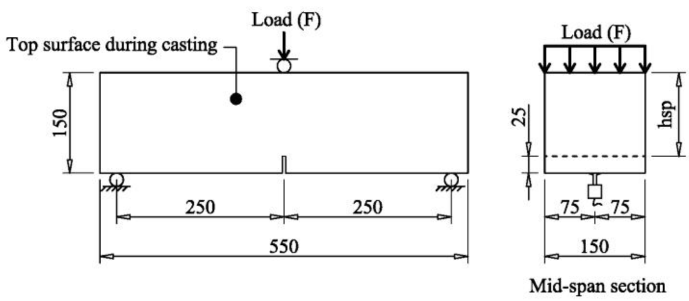

Figure 4. Typical arrangement of 3-point bending test over notched sample with measuring CMOD (EN 14651:2005)

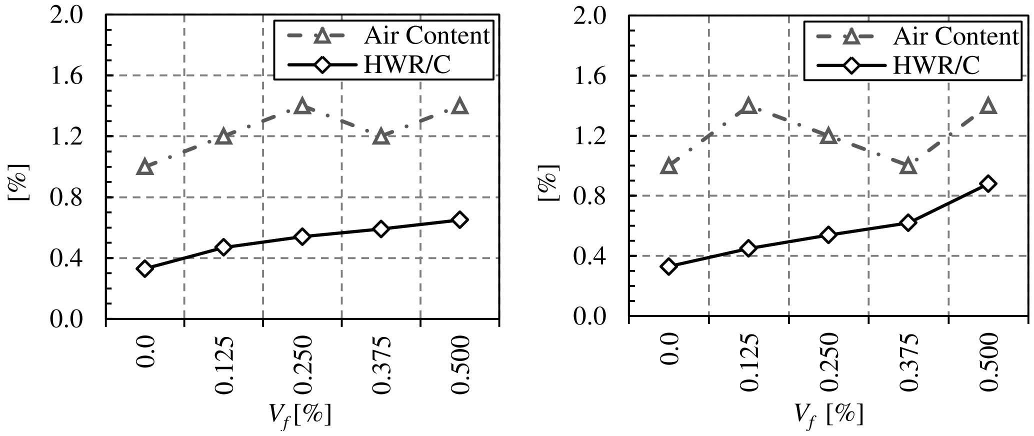

Figure 5. Air Content versus HWR/C for FRCs and control concrete - (a) FRCs with 6 mm fibres (b) FRCs with 12 mm fibres

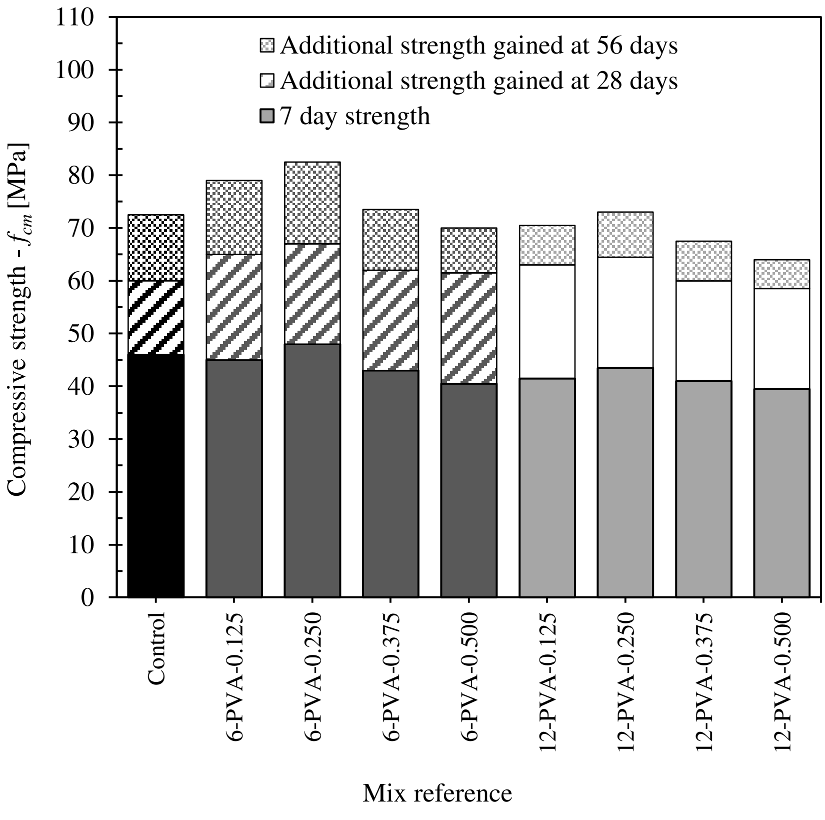

Figure 6. Compressive strength development from 7 to 28 and 56 days of FRCs versus control concrete

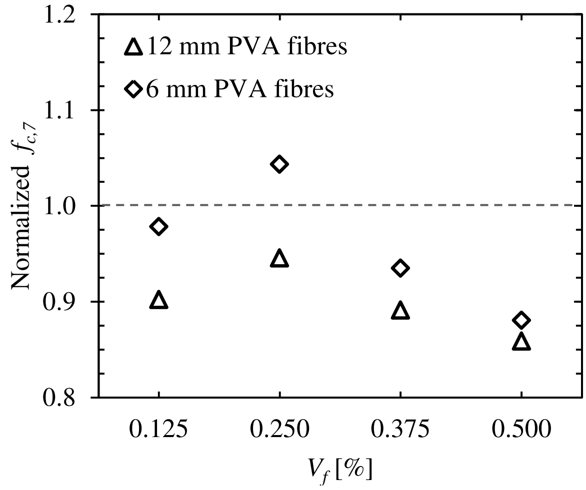

Figure 7. Normalized 7-day compressive strength of FRCs

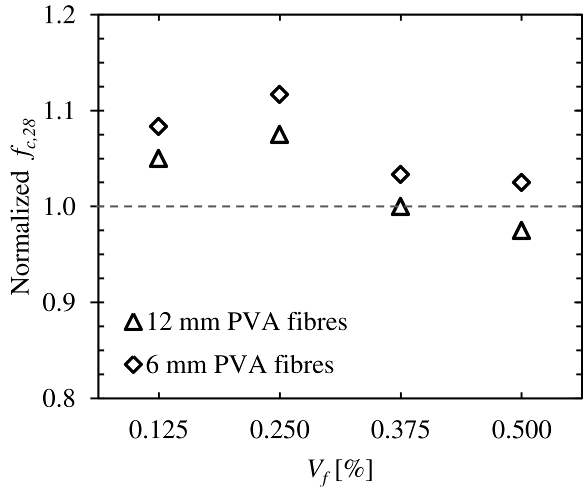

Figure 8. Normalized 28-day compressive strength of FRCs

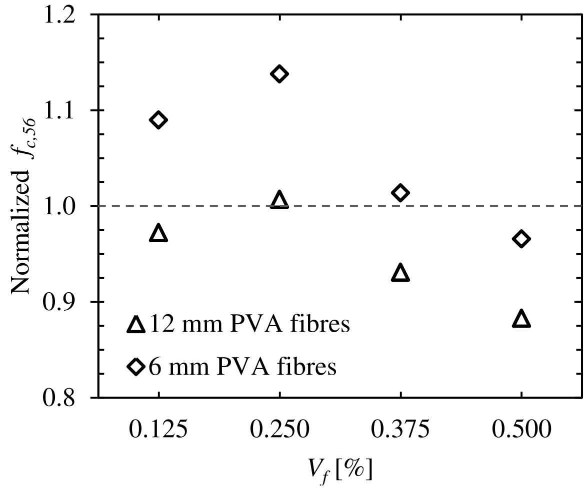

Figure 9. Normalized 56-day compressive strength of FRCs

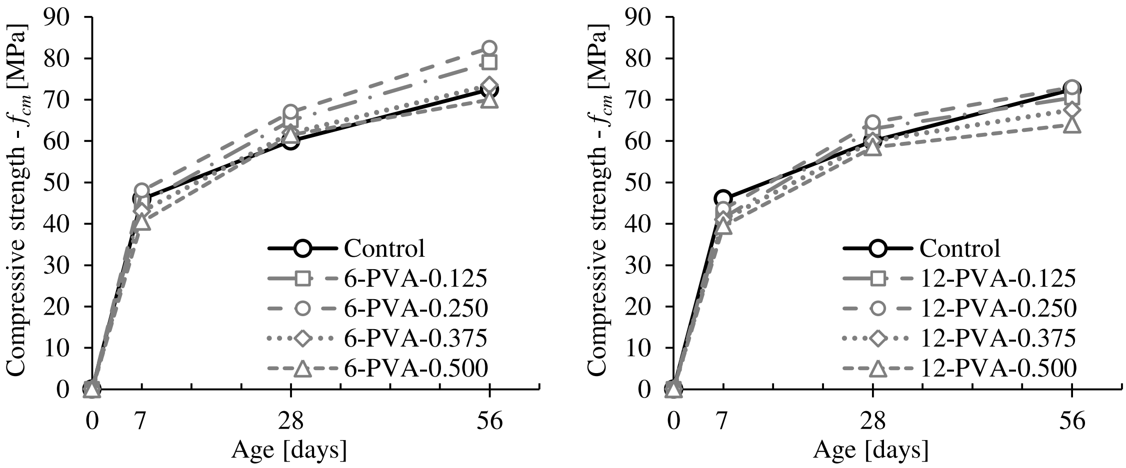

Figure 10. Compressive strength development of FRCs versus control concrete by ageing; FRCs with 6 mm fibres (left) FRCs with 12 mm fibres (right)

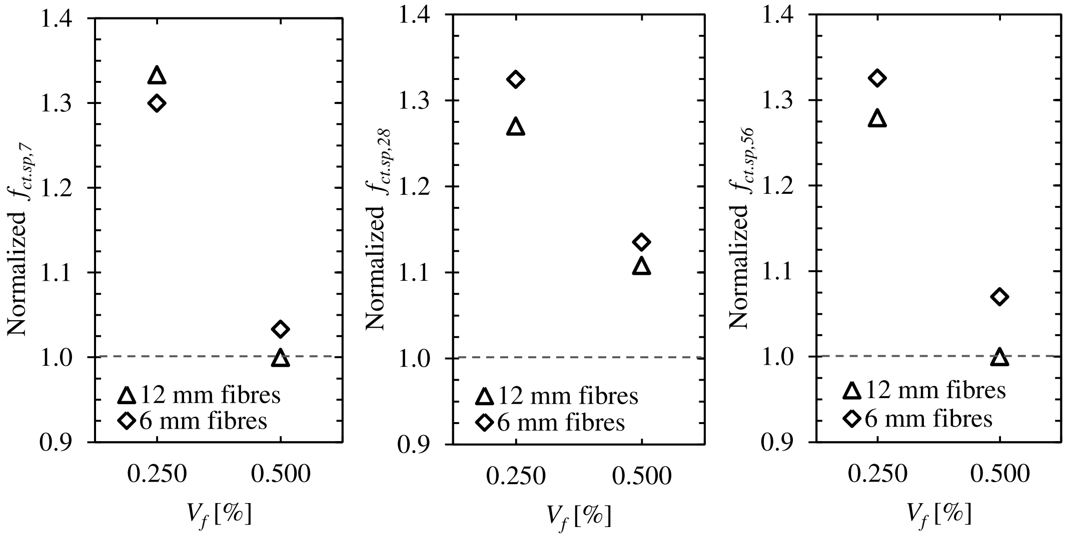

Figure 11. Normalized indirect tensile strength of FRCs after 7, 28 and 56 days

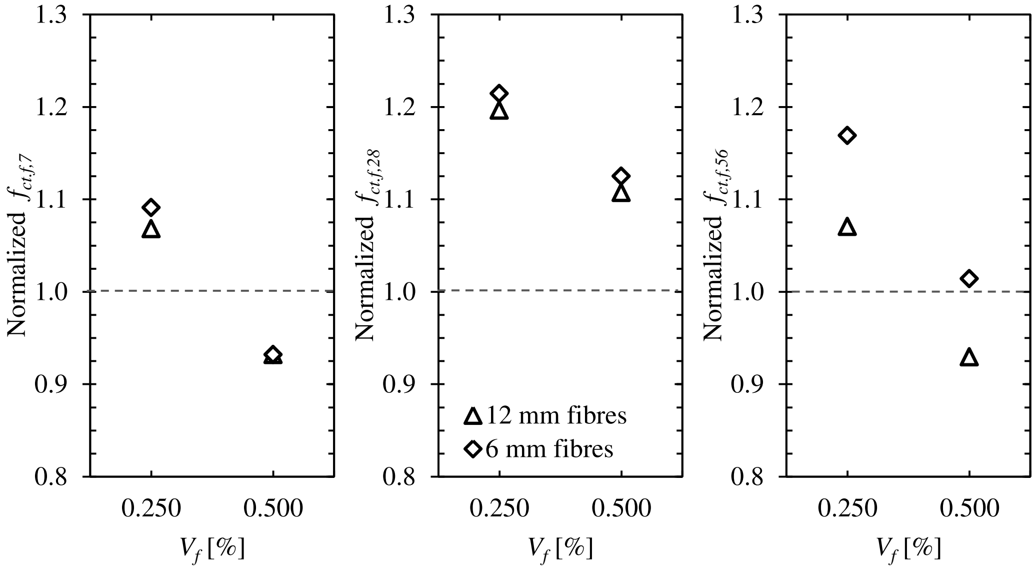

Figure 12. Normalized modulus of rupture of FRCs after 7, 28 and 56 days

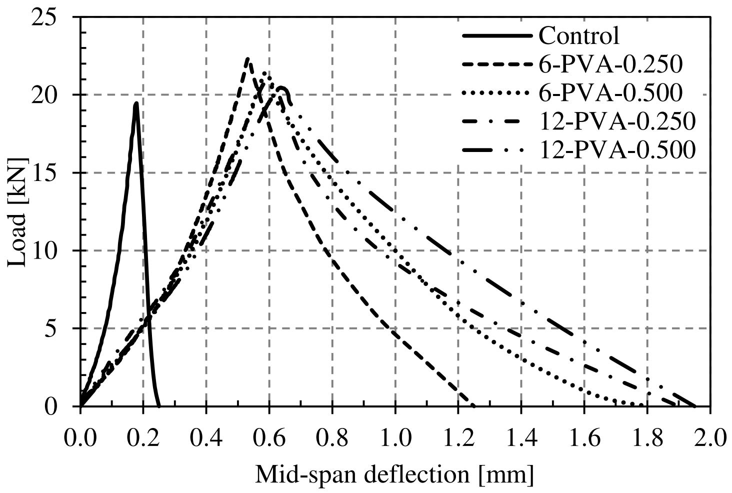

Figure 13. Load-mid span deflection curves in 28-day MOR test of control concrete and FRCs

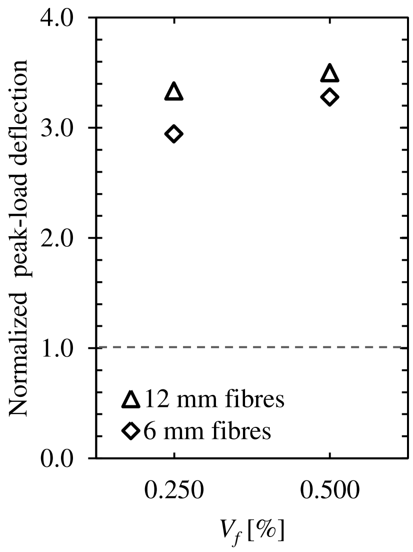

Figure 14. Normalized peak-load deflection of FRCs in 28-day MOR test

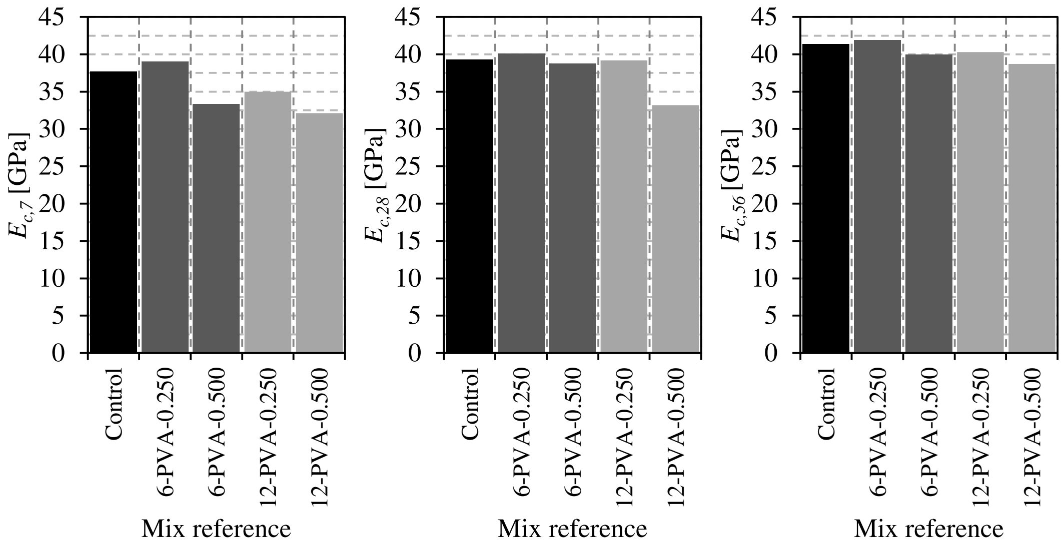

Figure 15. Elastic modulus of control concrete and FRCs after 7, 28 and 56 days

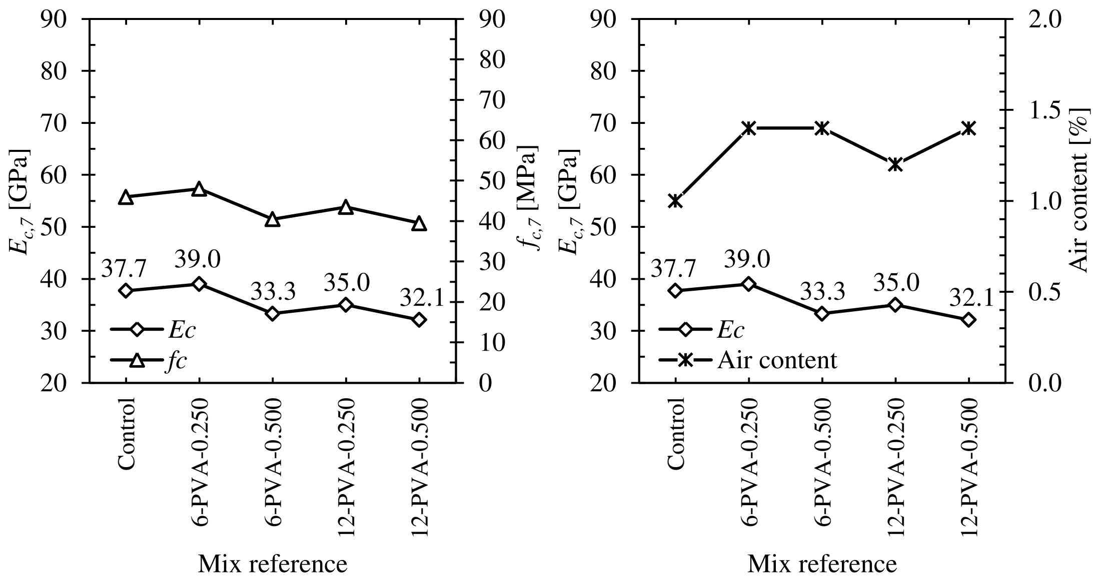

Figure 16. 7-day MOE versus 7-day compressive strength and air content

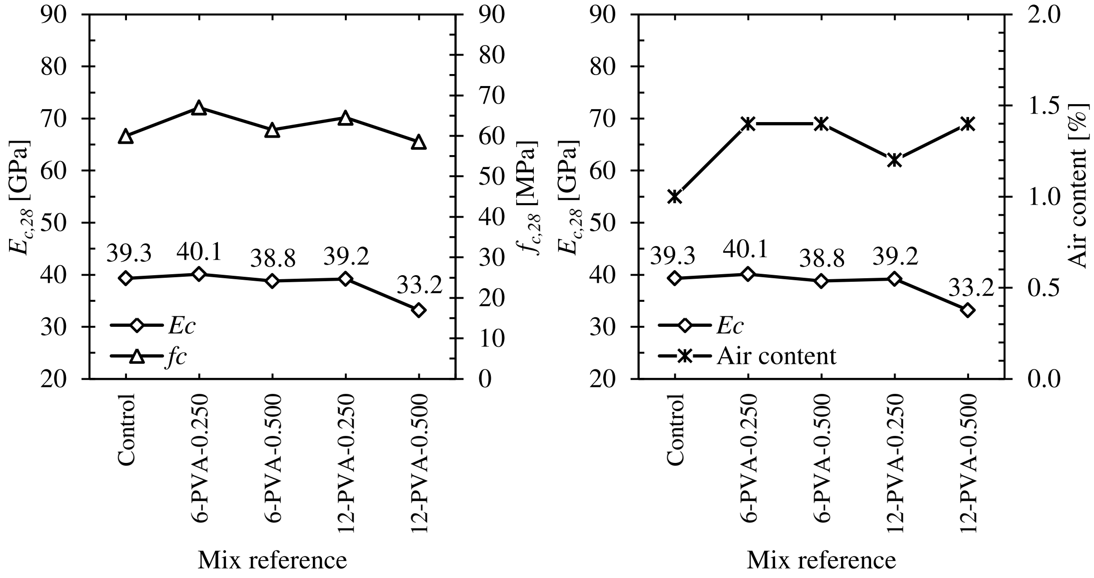

Figure 17. 28-day MOE versus 28-day compressive strength and air content

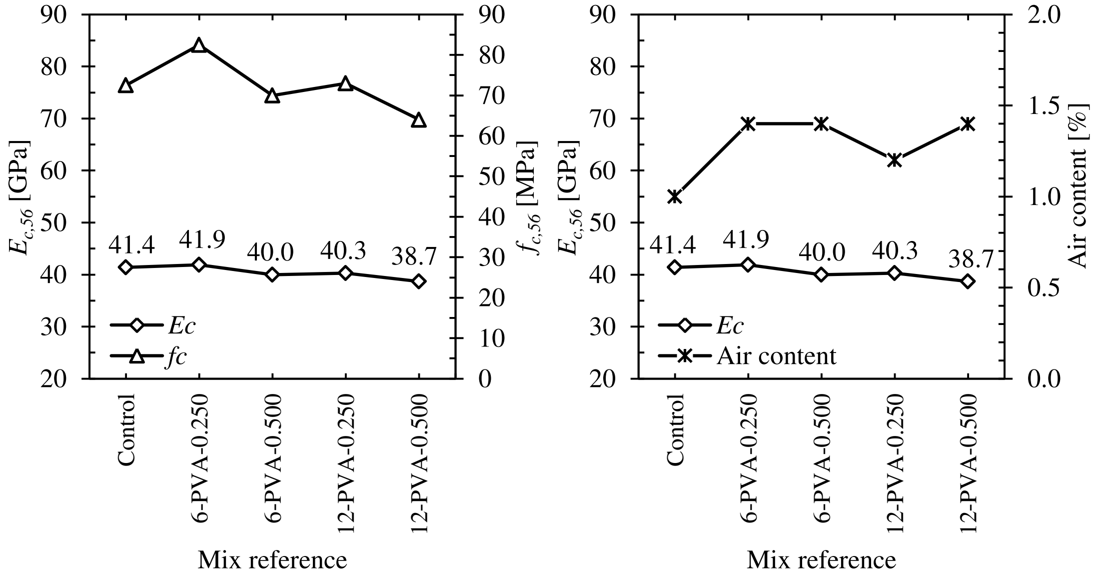

Figure 18. 56-day MOE versus 56-day compressive strength and air content

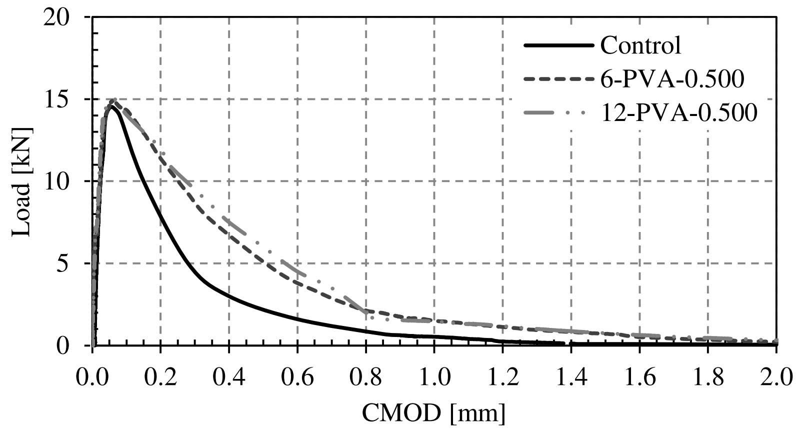

Figure 19. Load-CMOD curves of FRCs versus control concrete

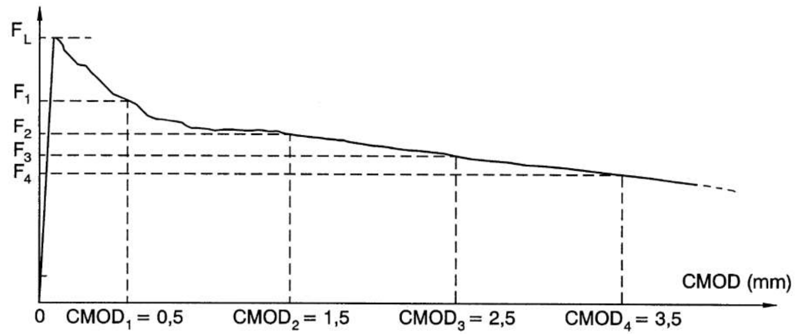

Figure 20. Typical Load-CMOD curve and definition of the reference points on the curve (EN 14651:2005)

Figure 1
Click here to download high resolution image

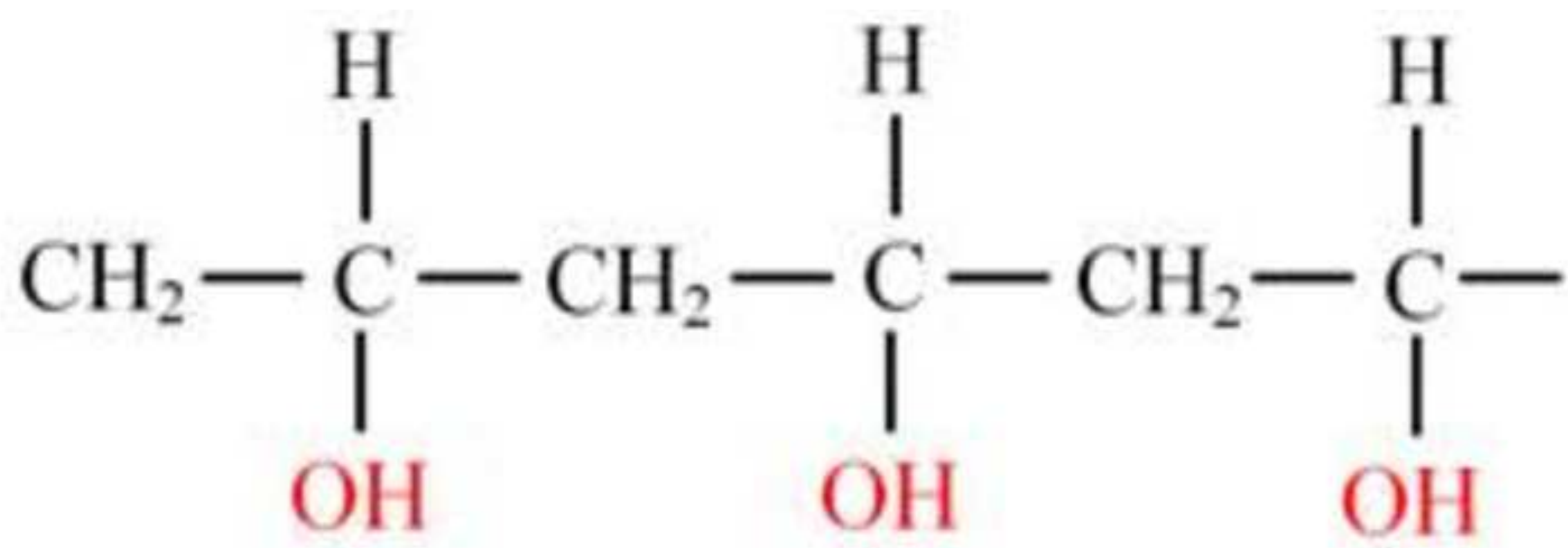

Figure 2
Click here to download high resolution image

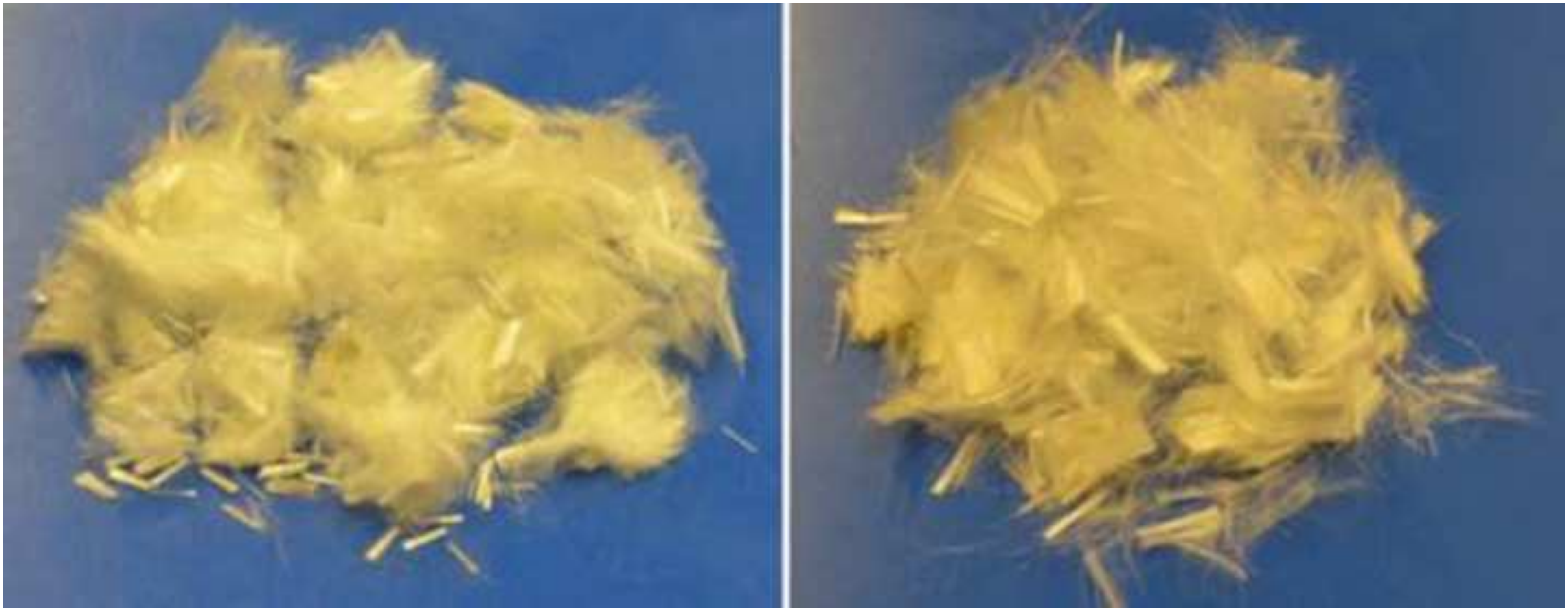

Figure 3
Click here to download high resolution image

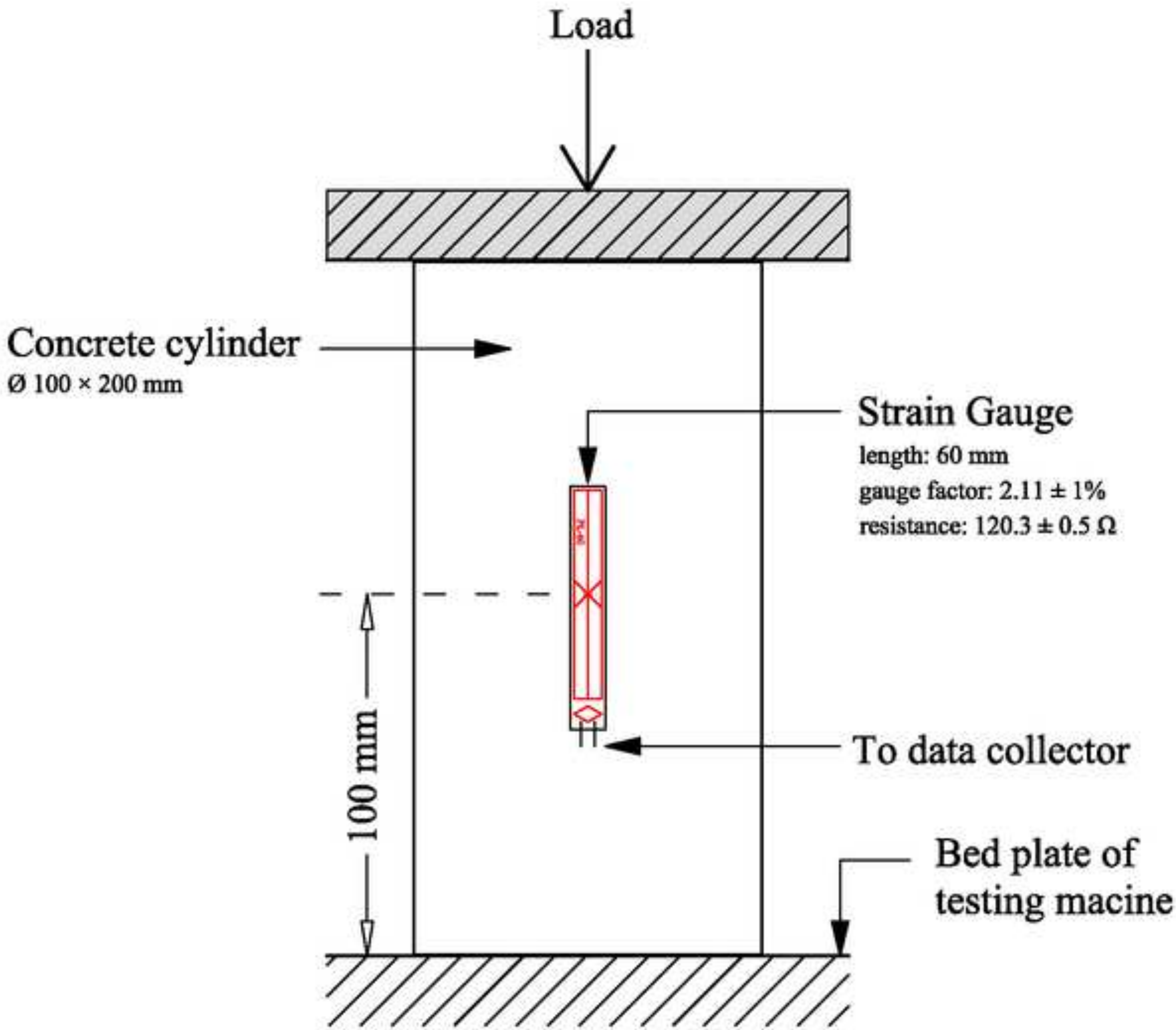

Figure 4
Click here to download high resolution image

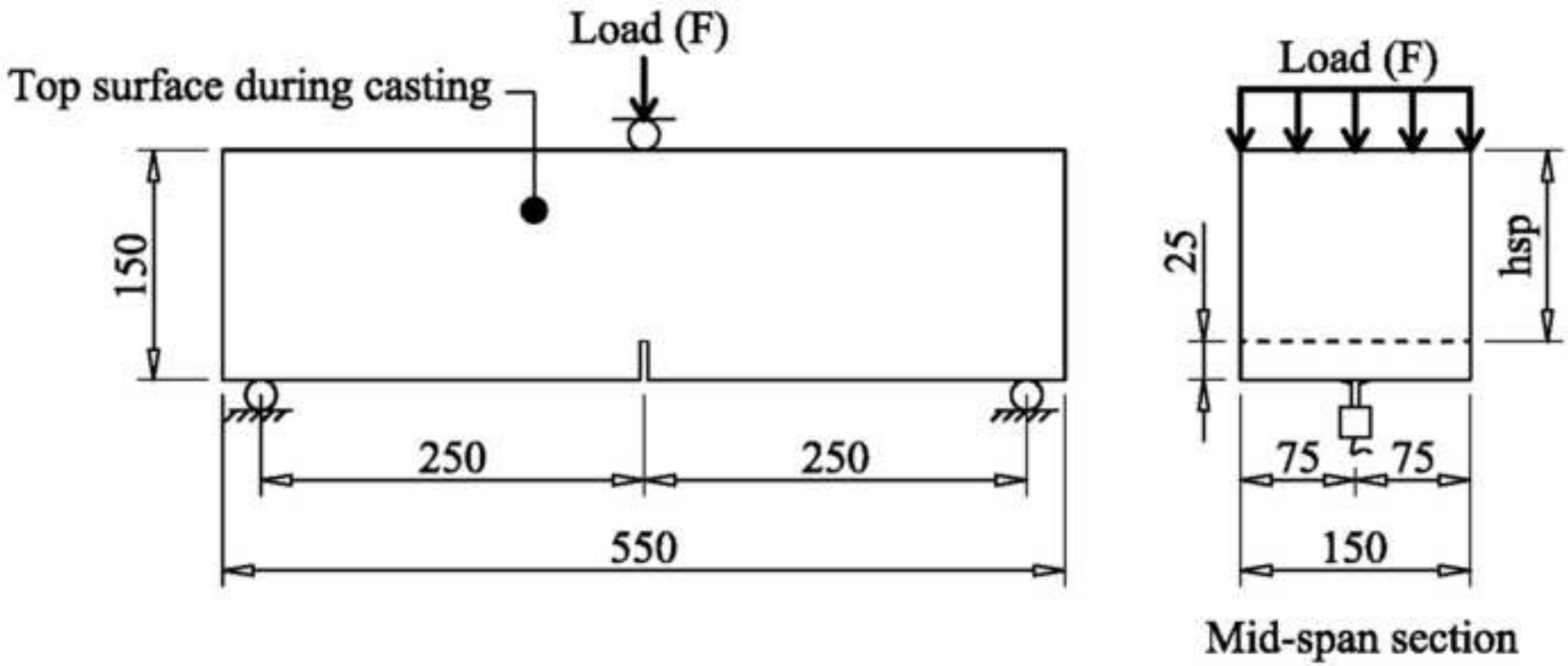

Figure 5a
Click here to download high resolution image

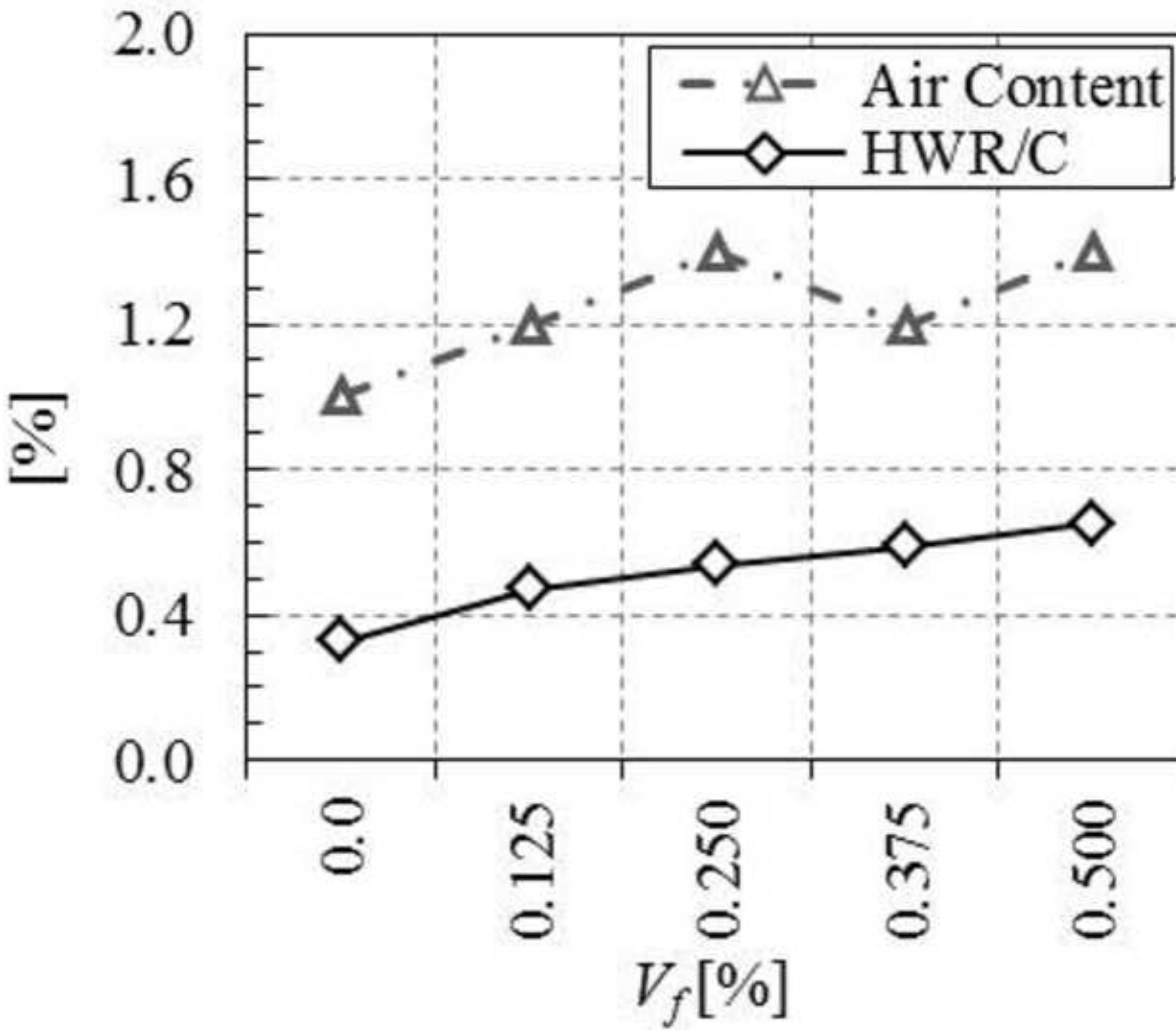

Figure 5b
Click here to download high resolution image

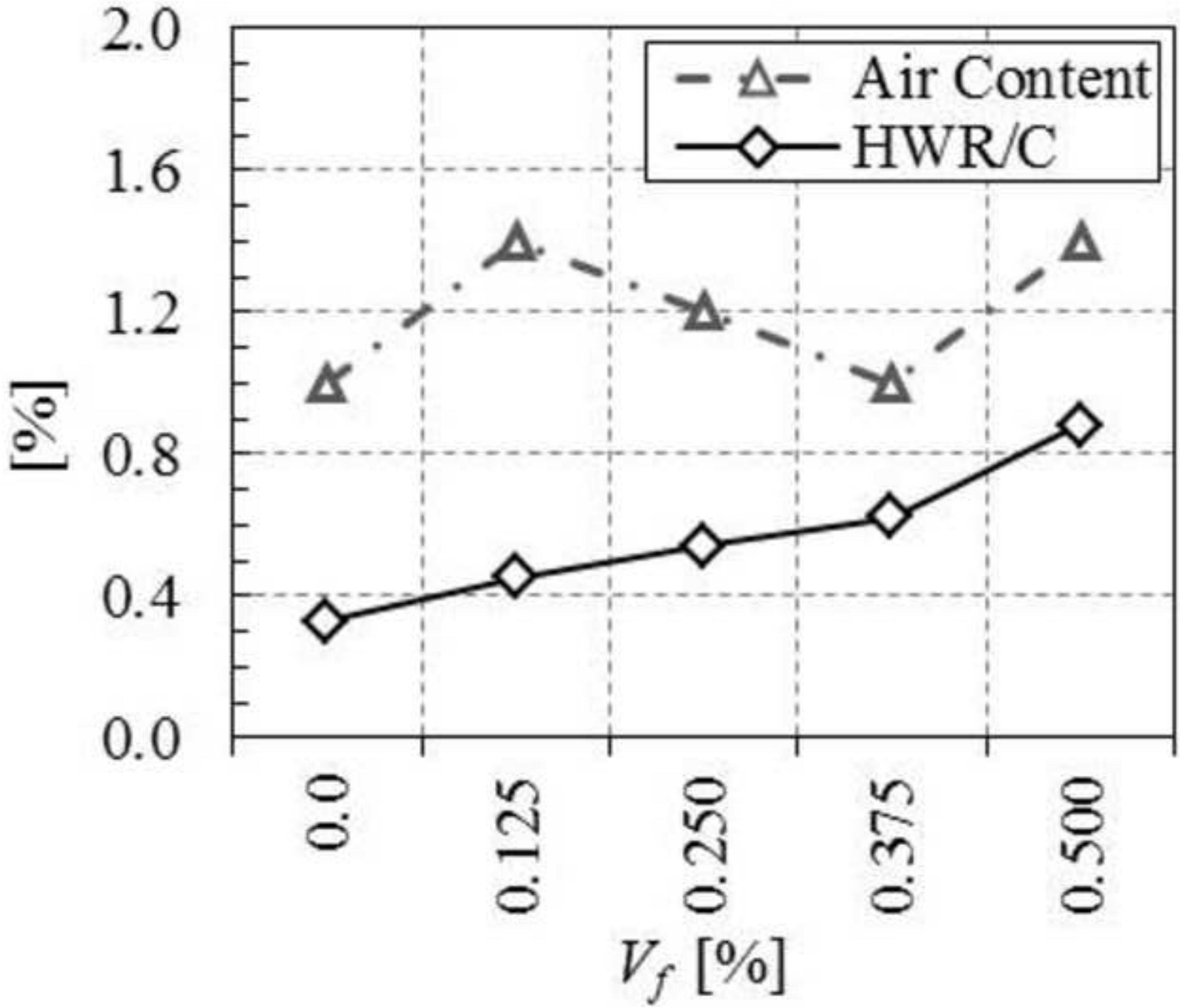

Figure 6

Click here to download high resolution image

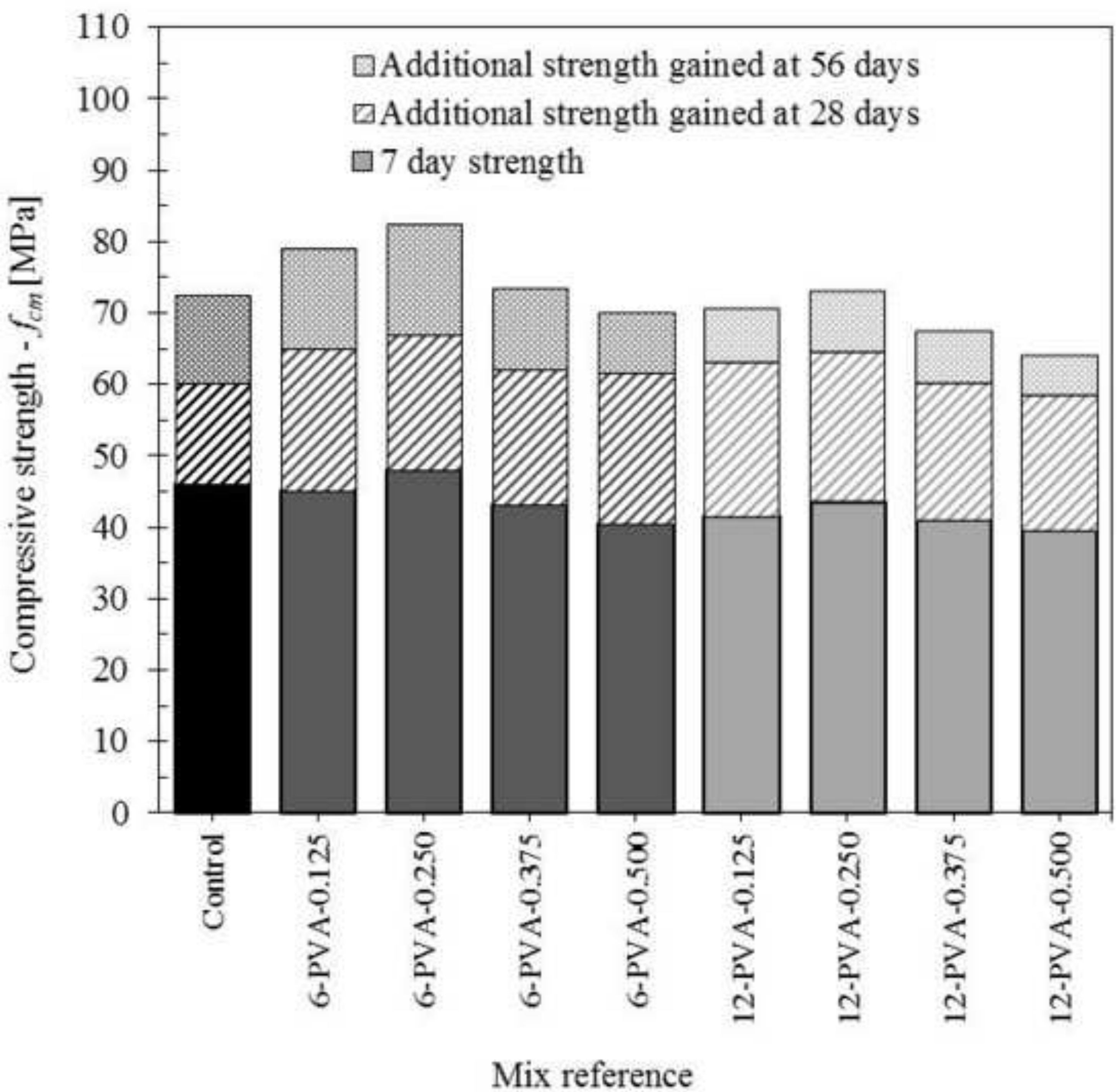

Figure 7
Click here to download high resolution image

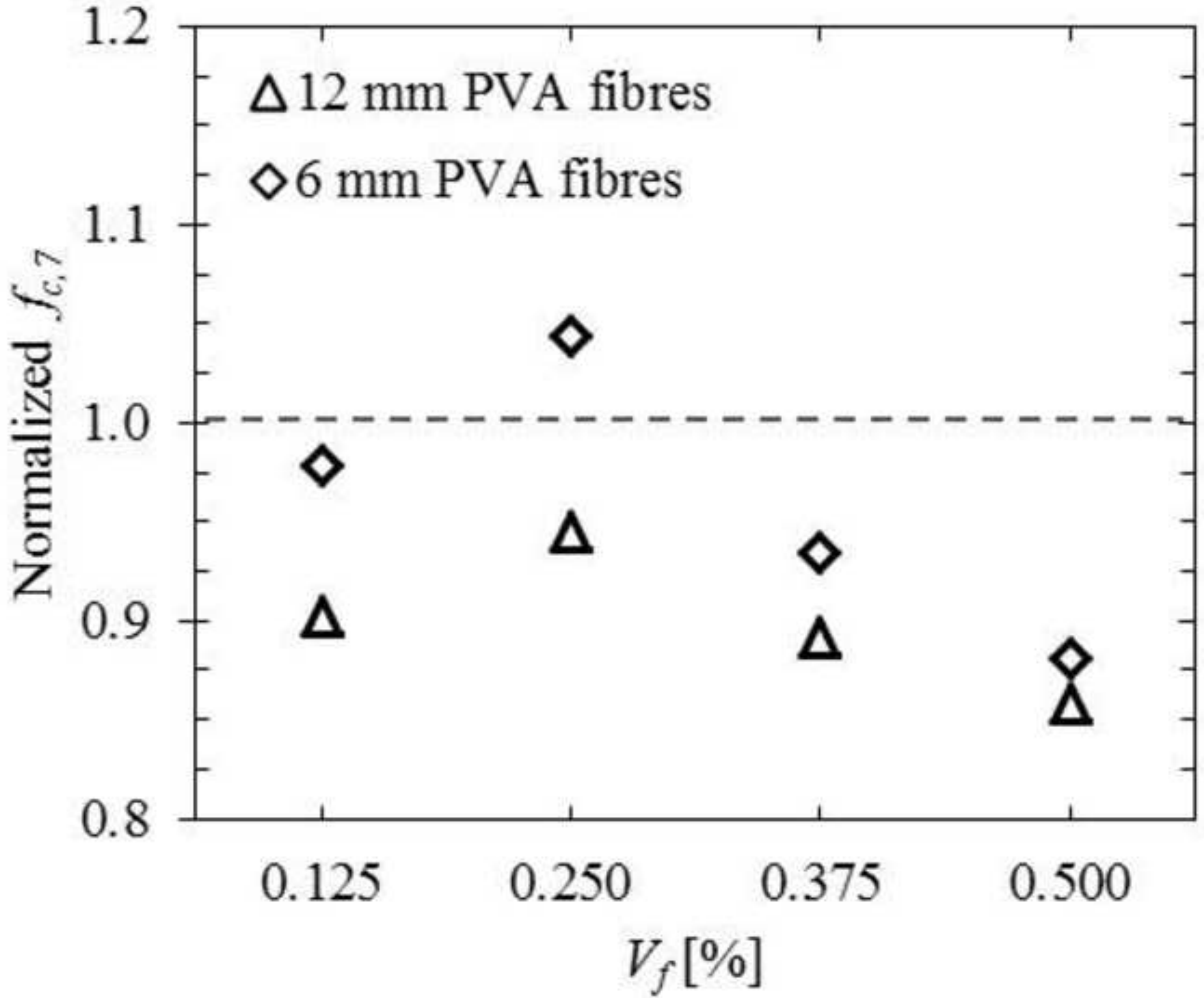

Figure 8
Click here to download high resolution image

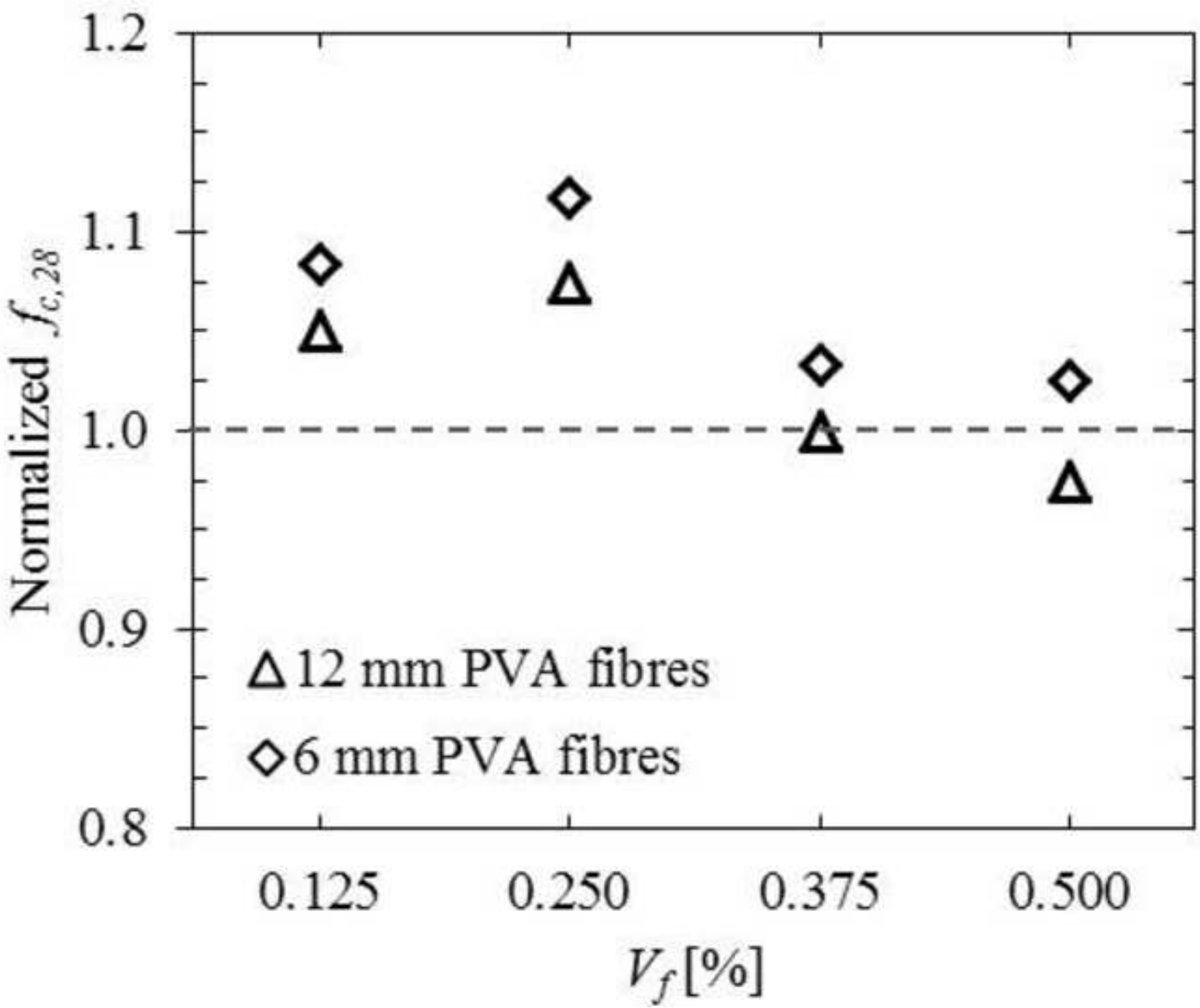

Figure 9

Click here to download high resolution image

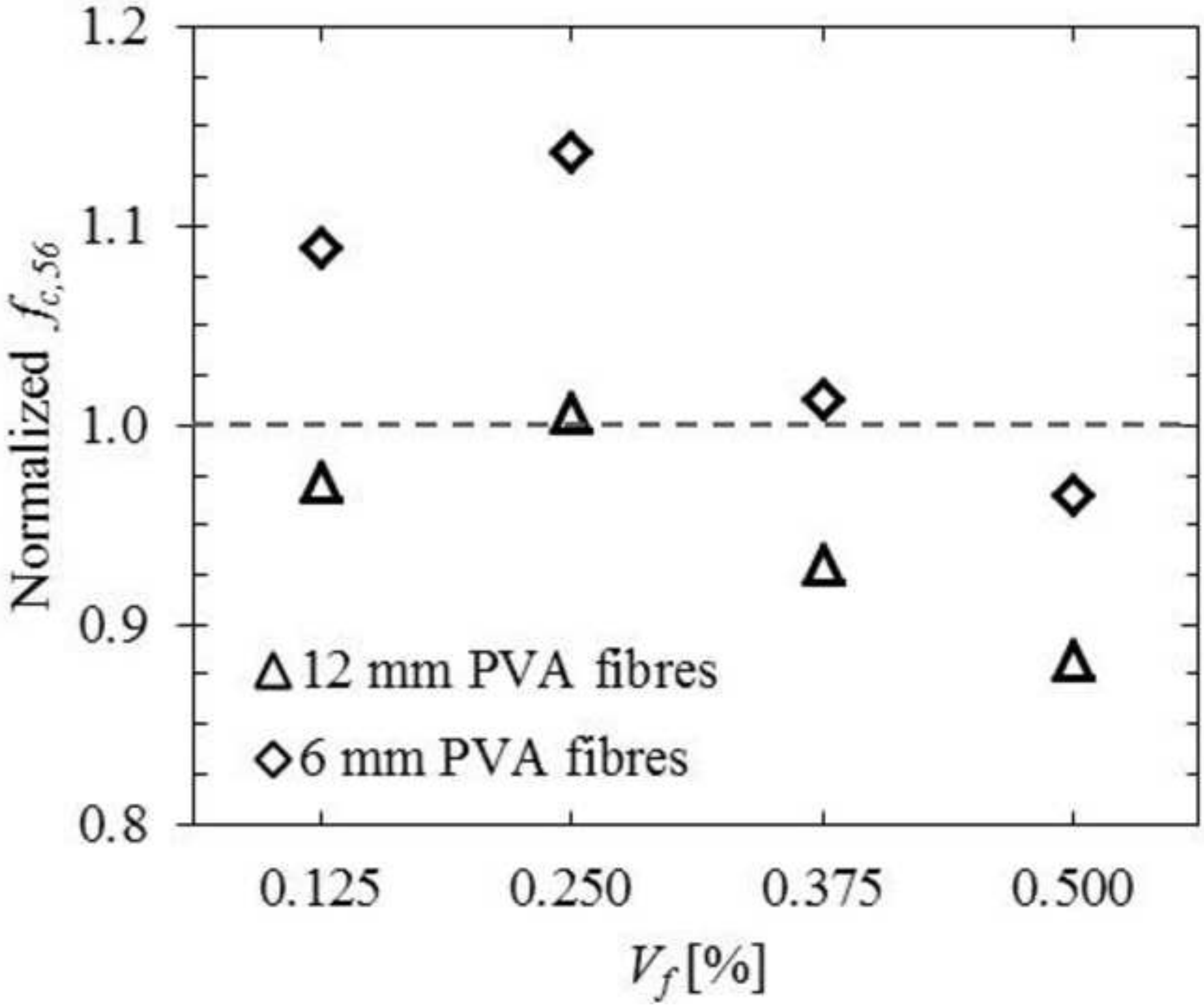

Figure 10a
Click here to download high resolution image

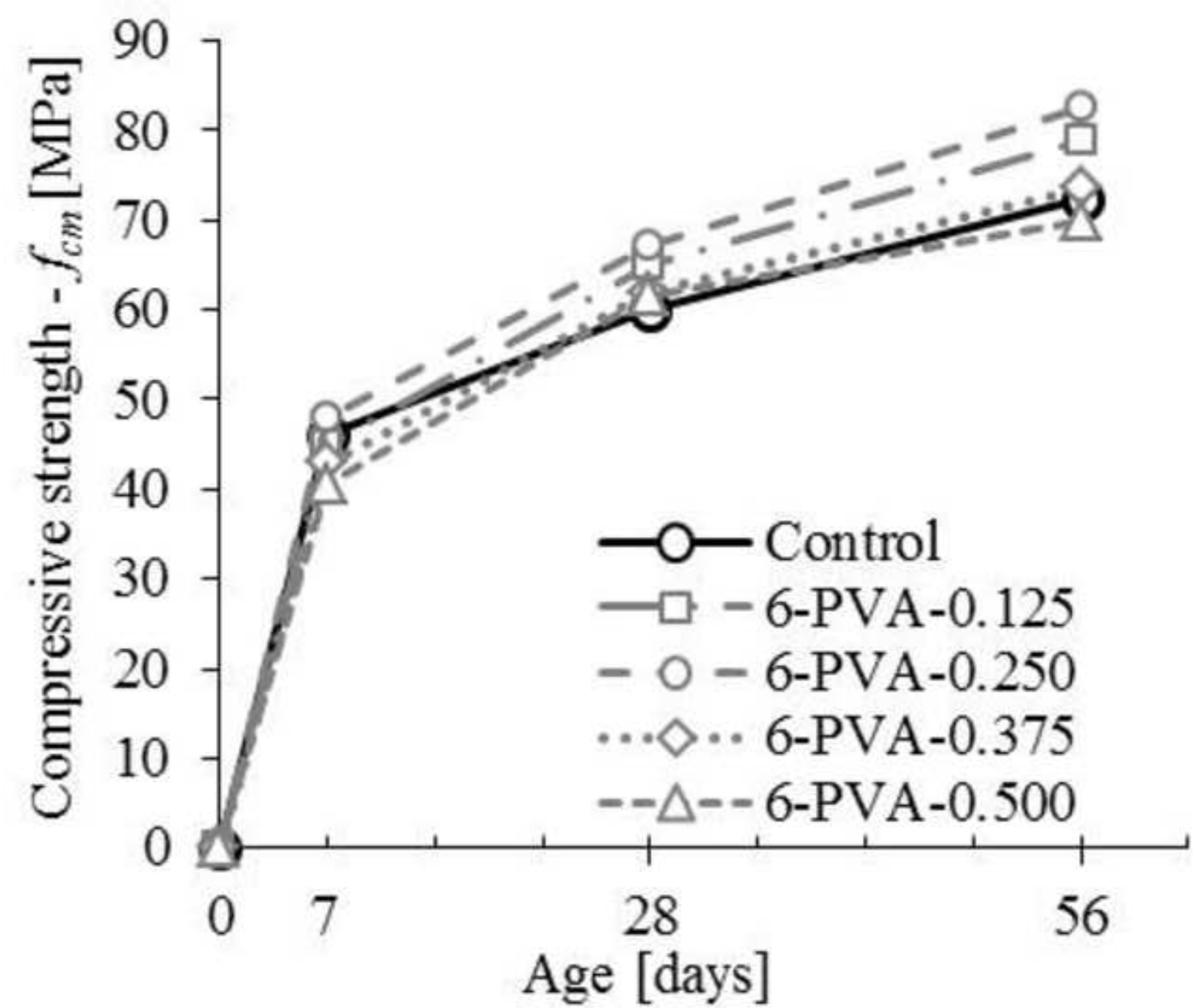

Figure 10b
Click here to download high resolution image

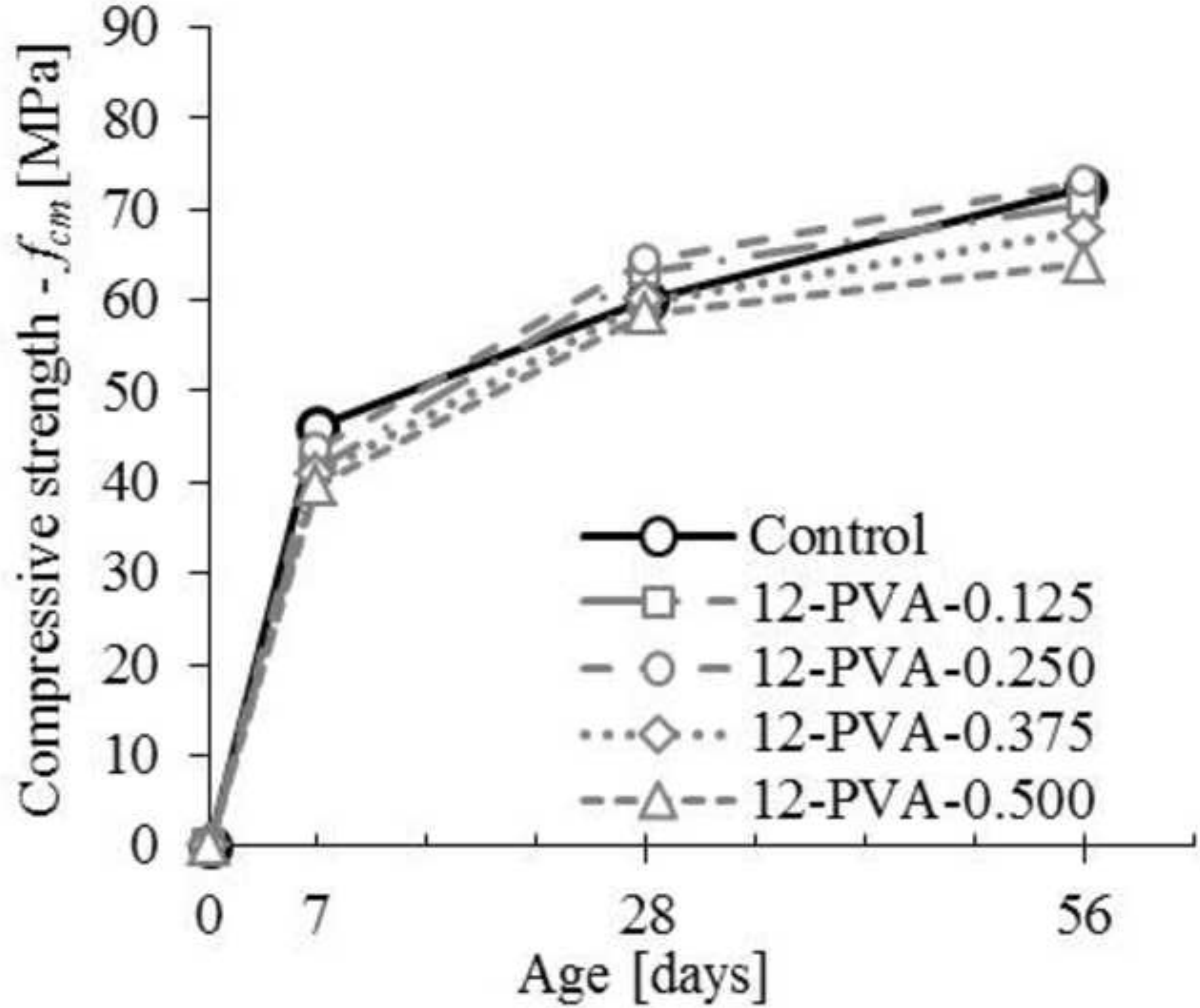

Figure 11a
Click here to download high resolution image

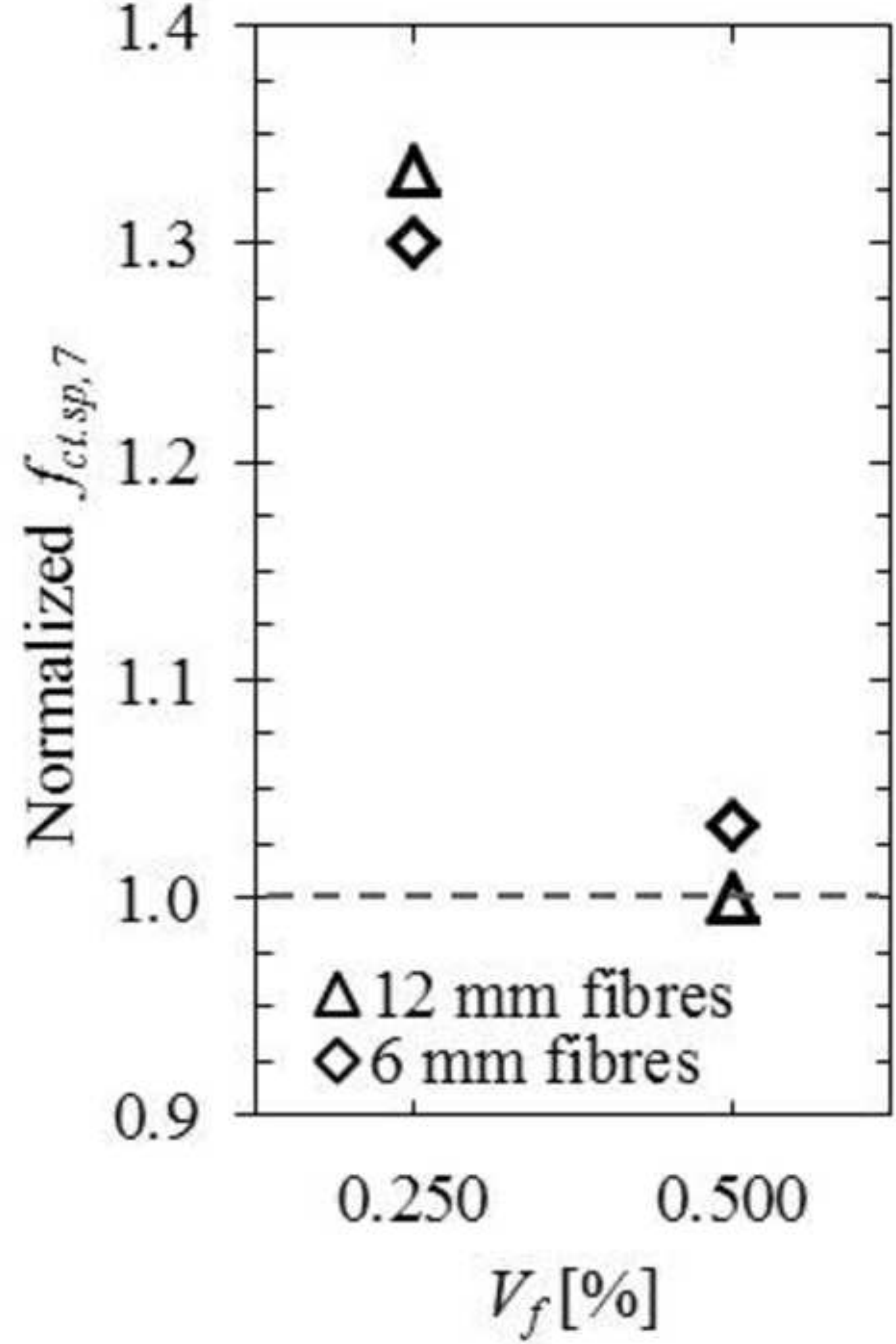

Figure 11b
Click here to download high resolution image

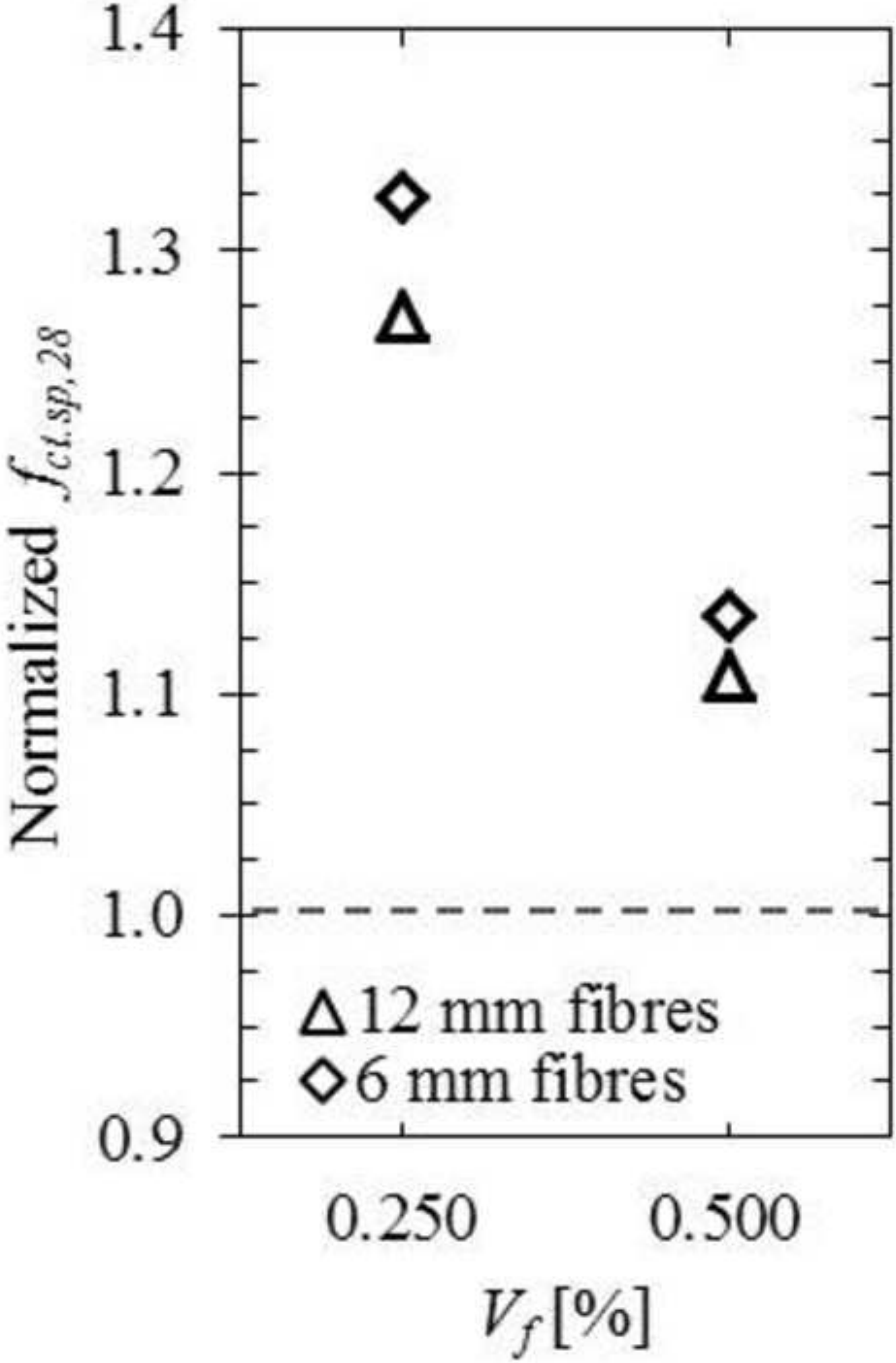

Figure 11c
Click here to download high resolution image

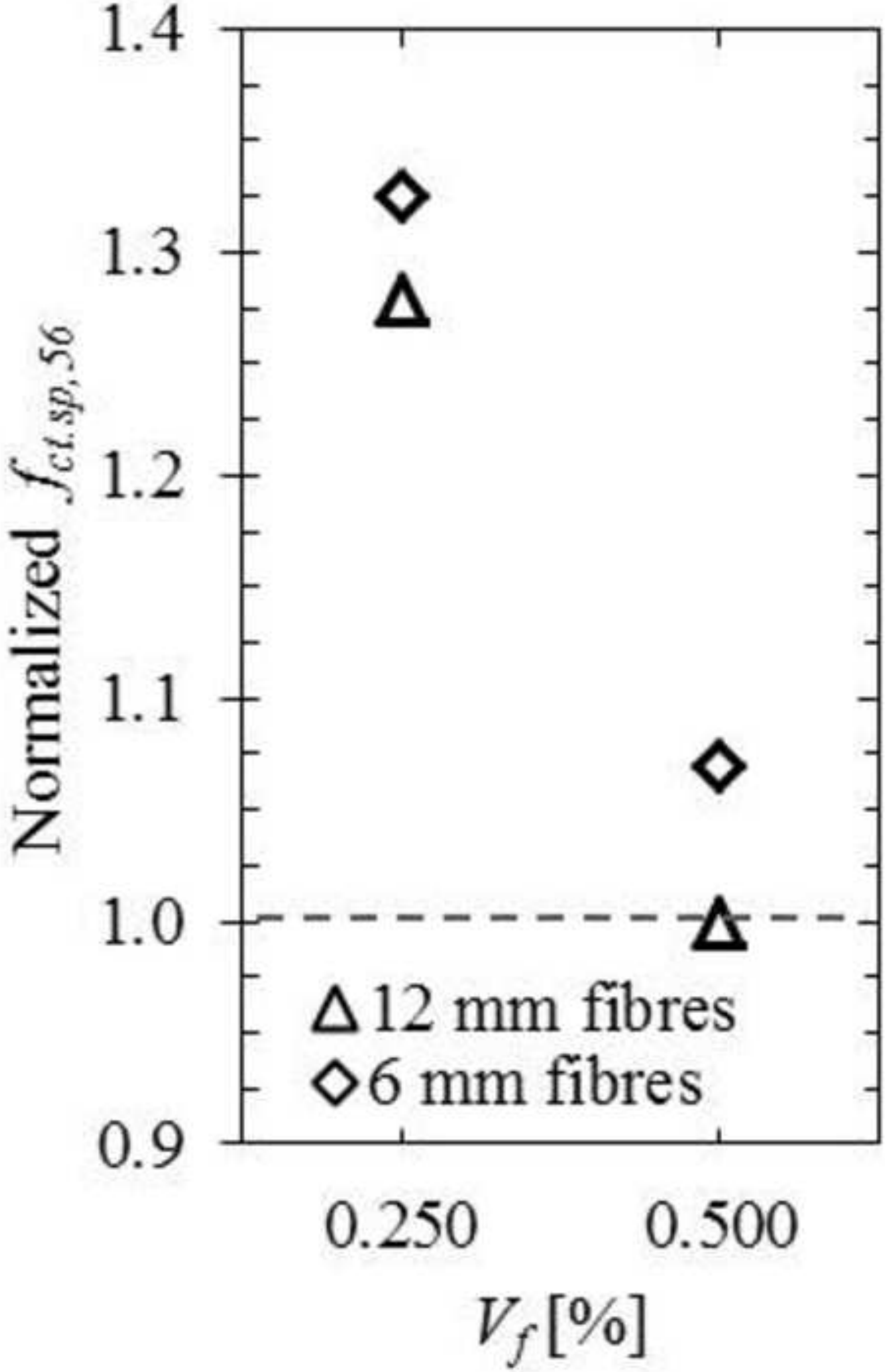

Figure 12a
Click here to download high resolution image

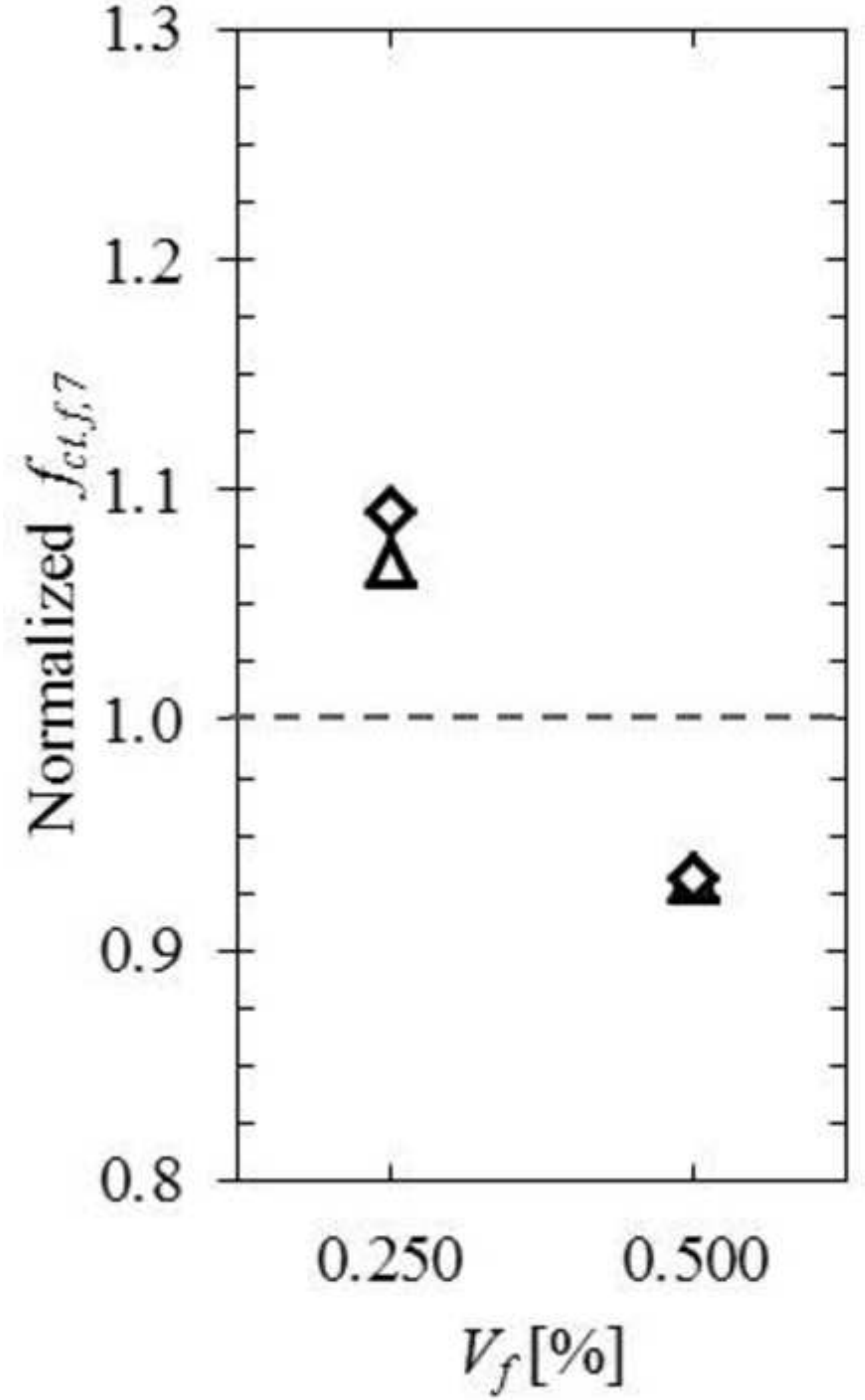

Figure 12b
Click here to download high resolution image

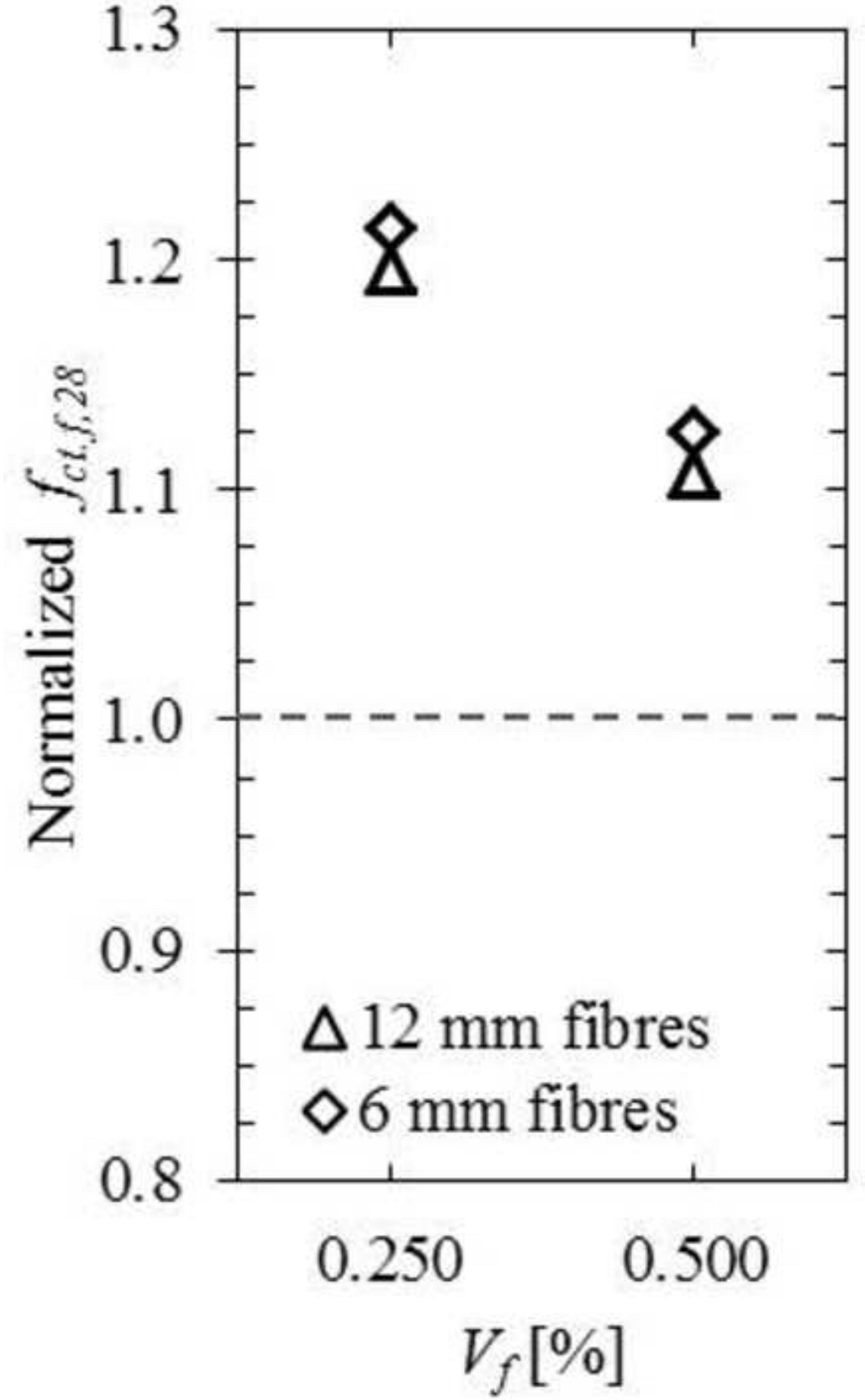

Figure 12c
Click here to download high resolution image

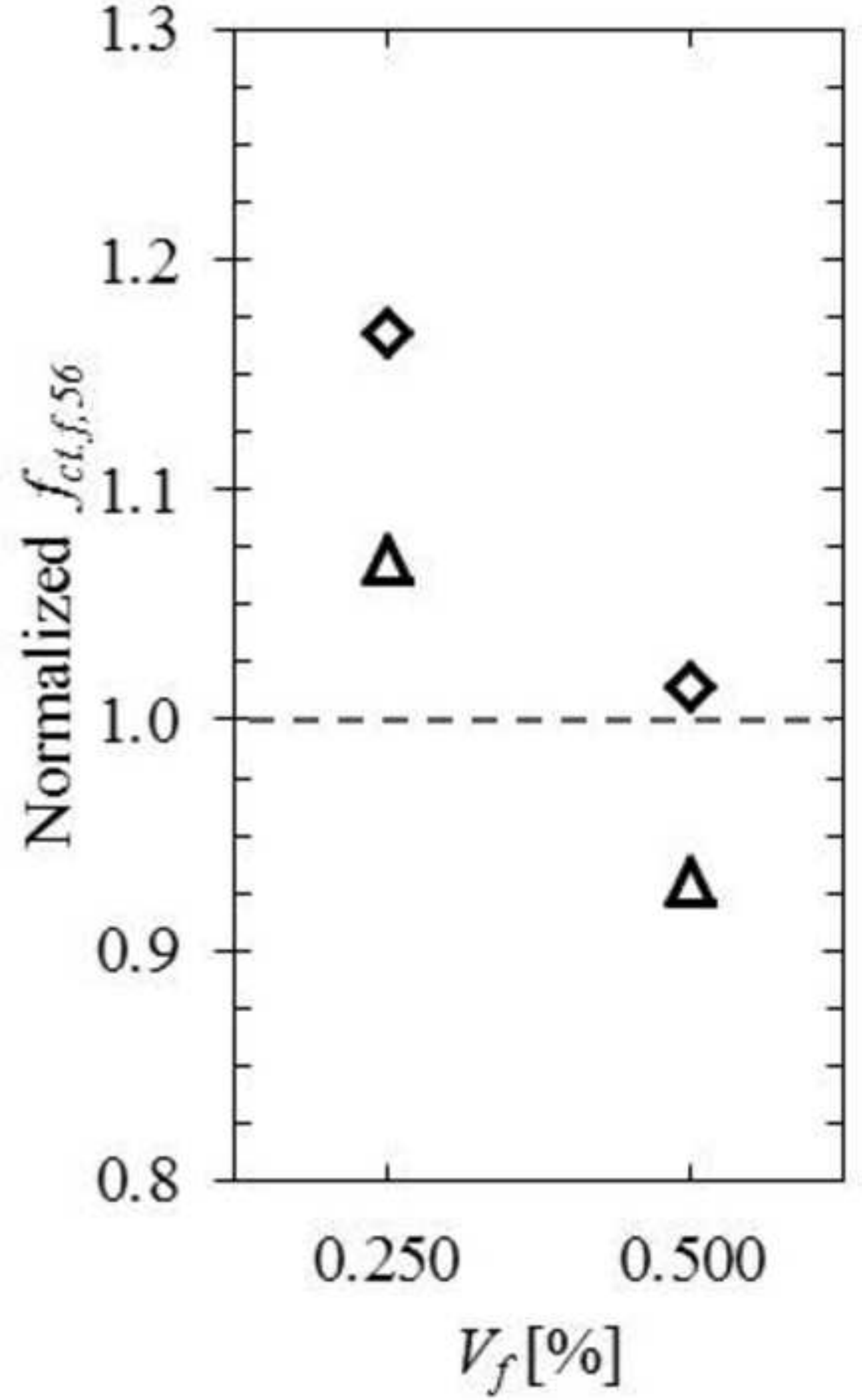

Figure 13
Click here to download high resolution image

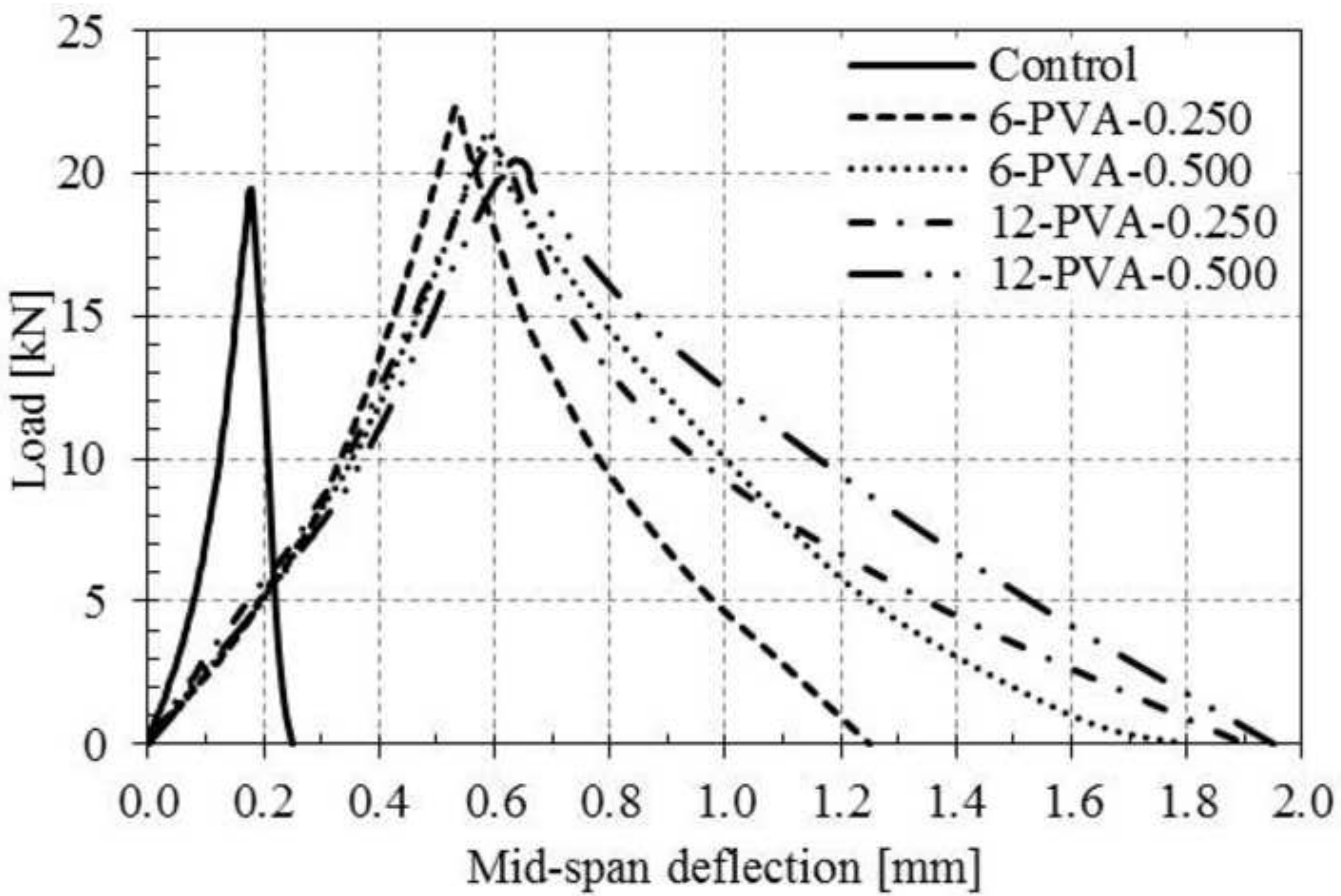

Figure 14
Click here to download high resolution image

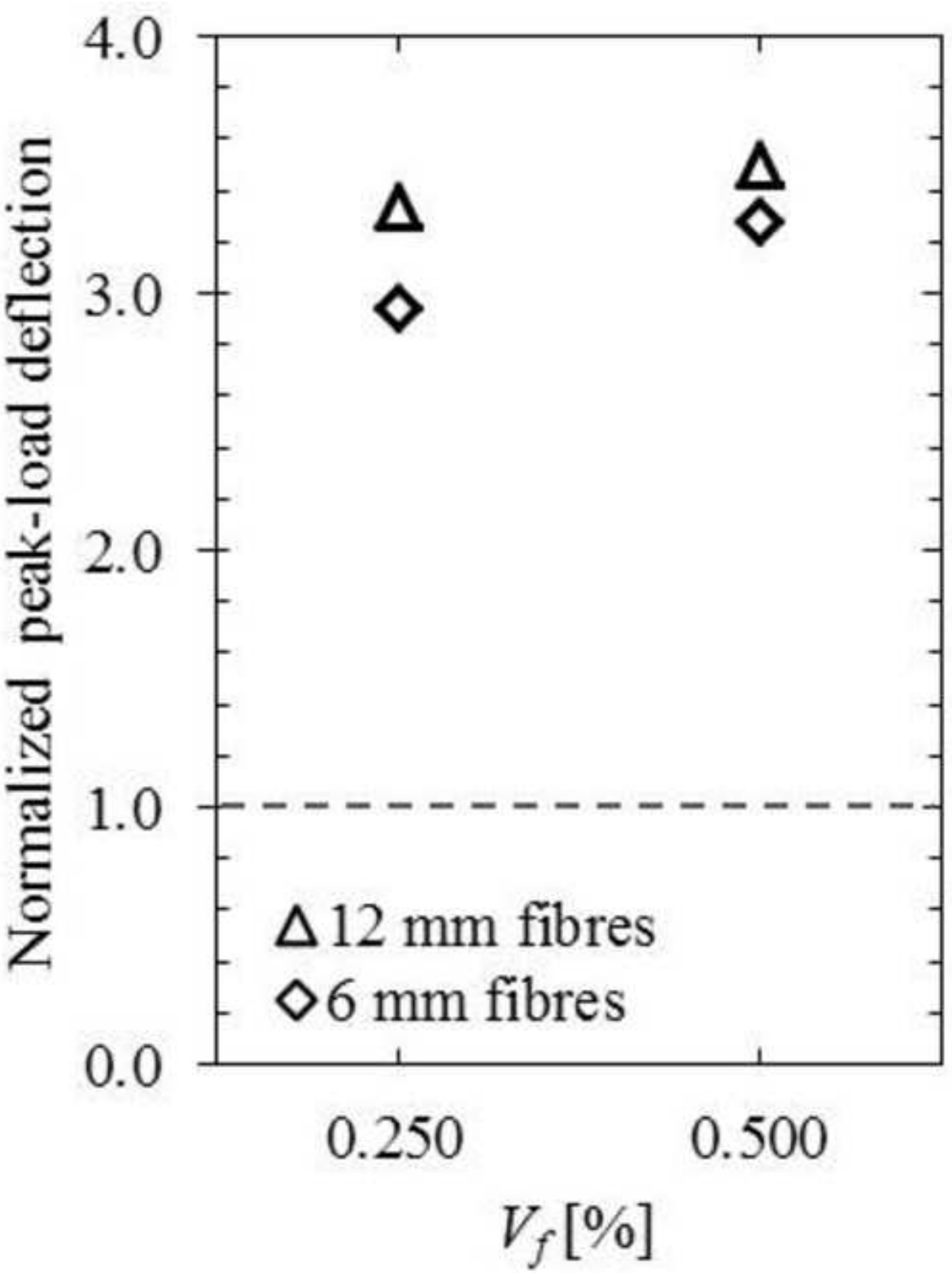

Figure 15a
Click here to download high resolution image

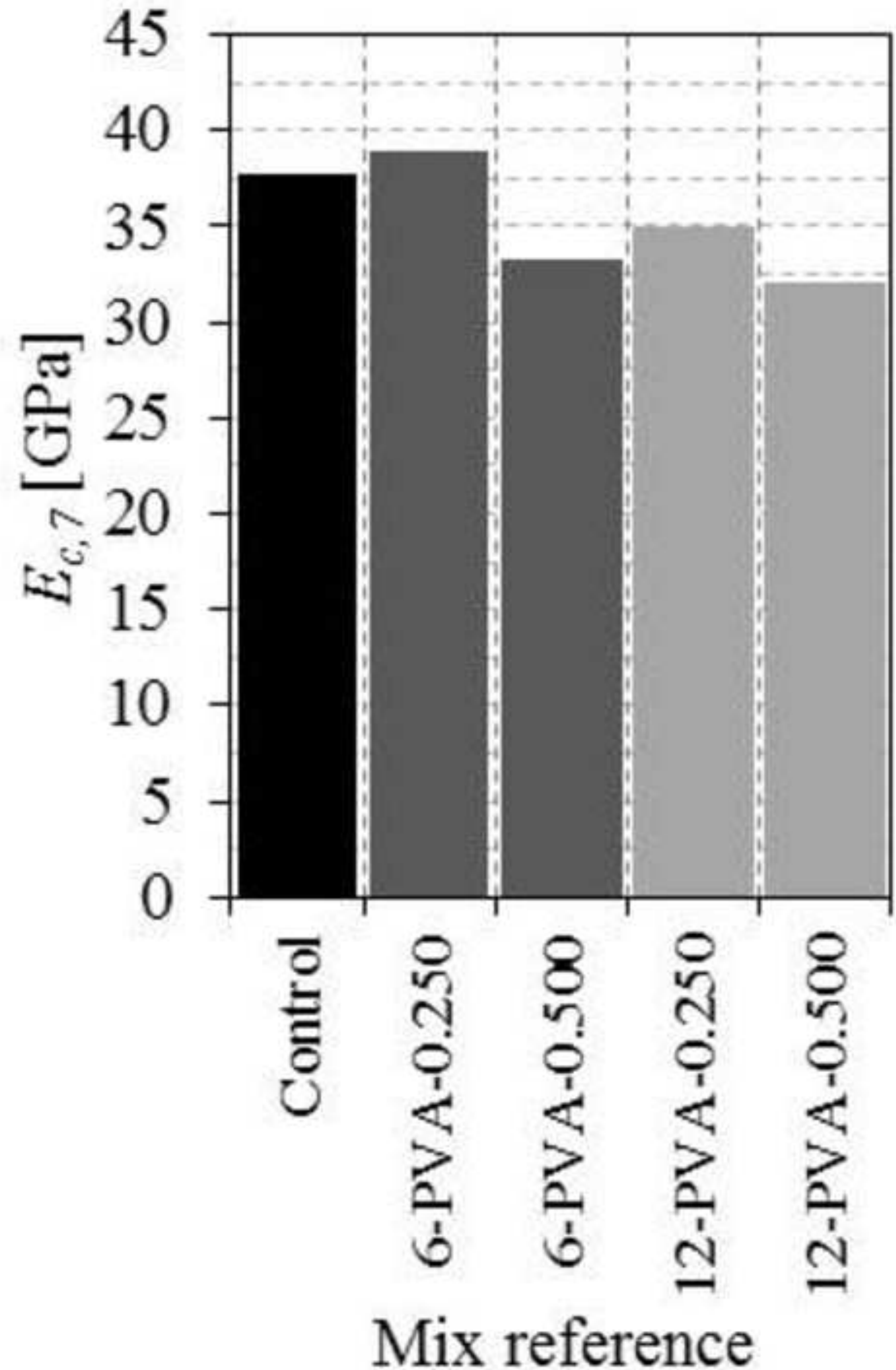

Figure 15b
Click here to download high resolution image

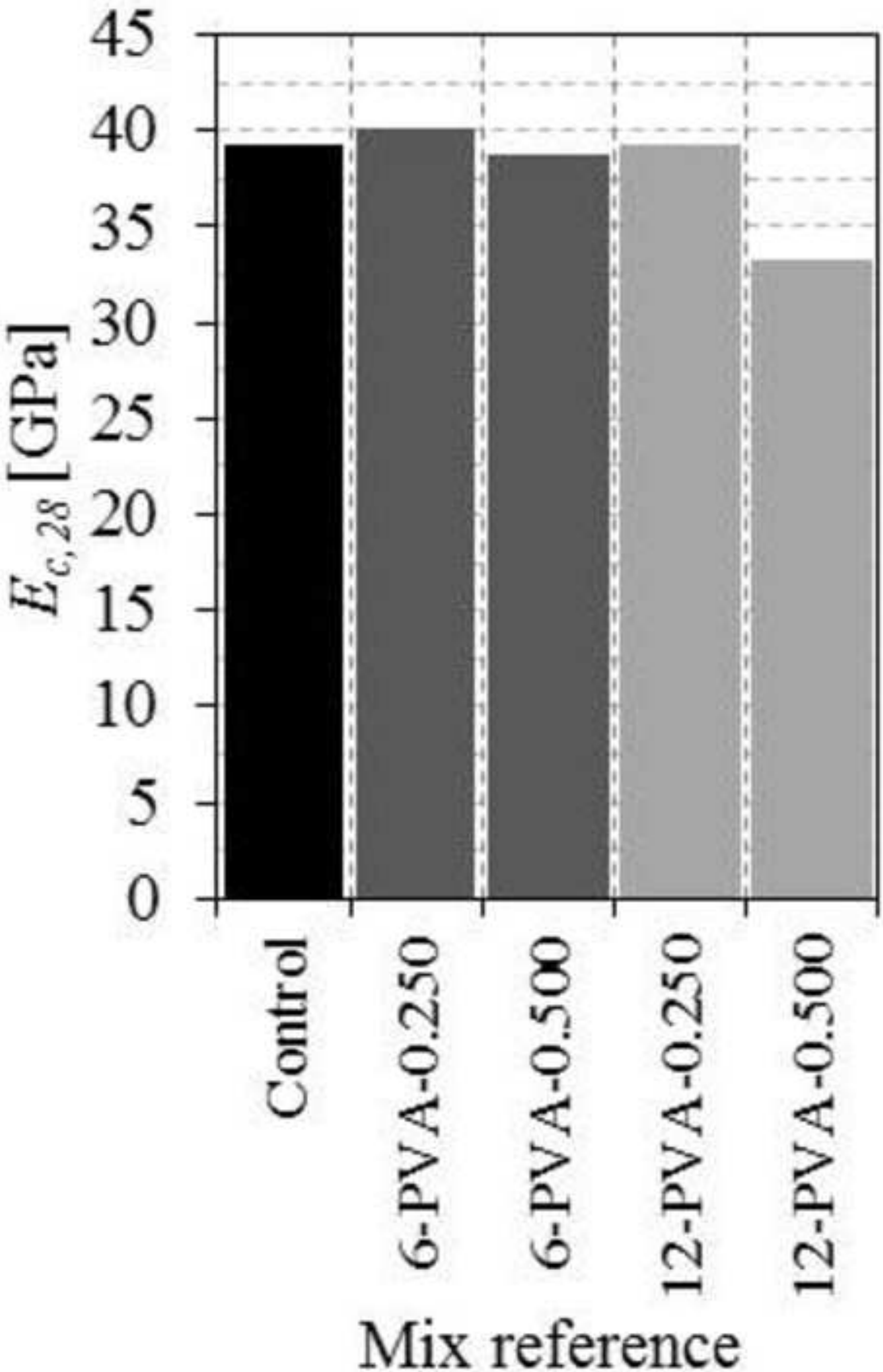

Figure 15c
Click here to download high resolution image

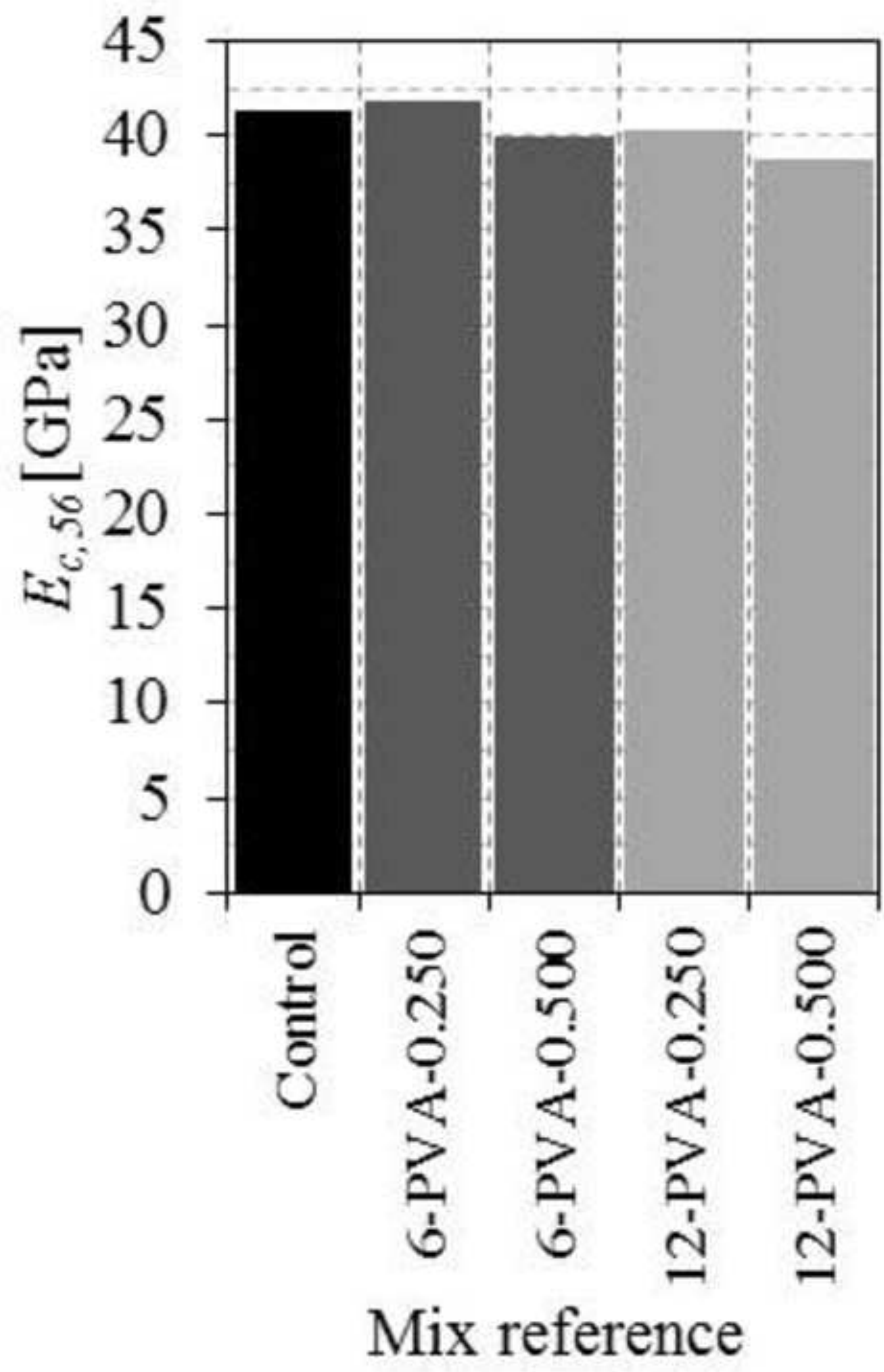

Figure 16a
Click here to download high resolution image

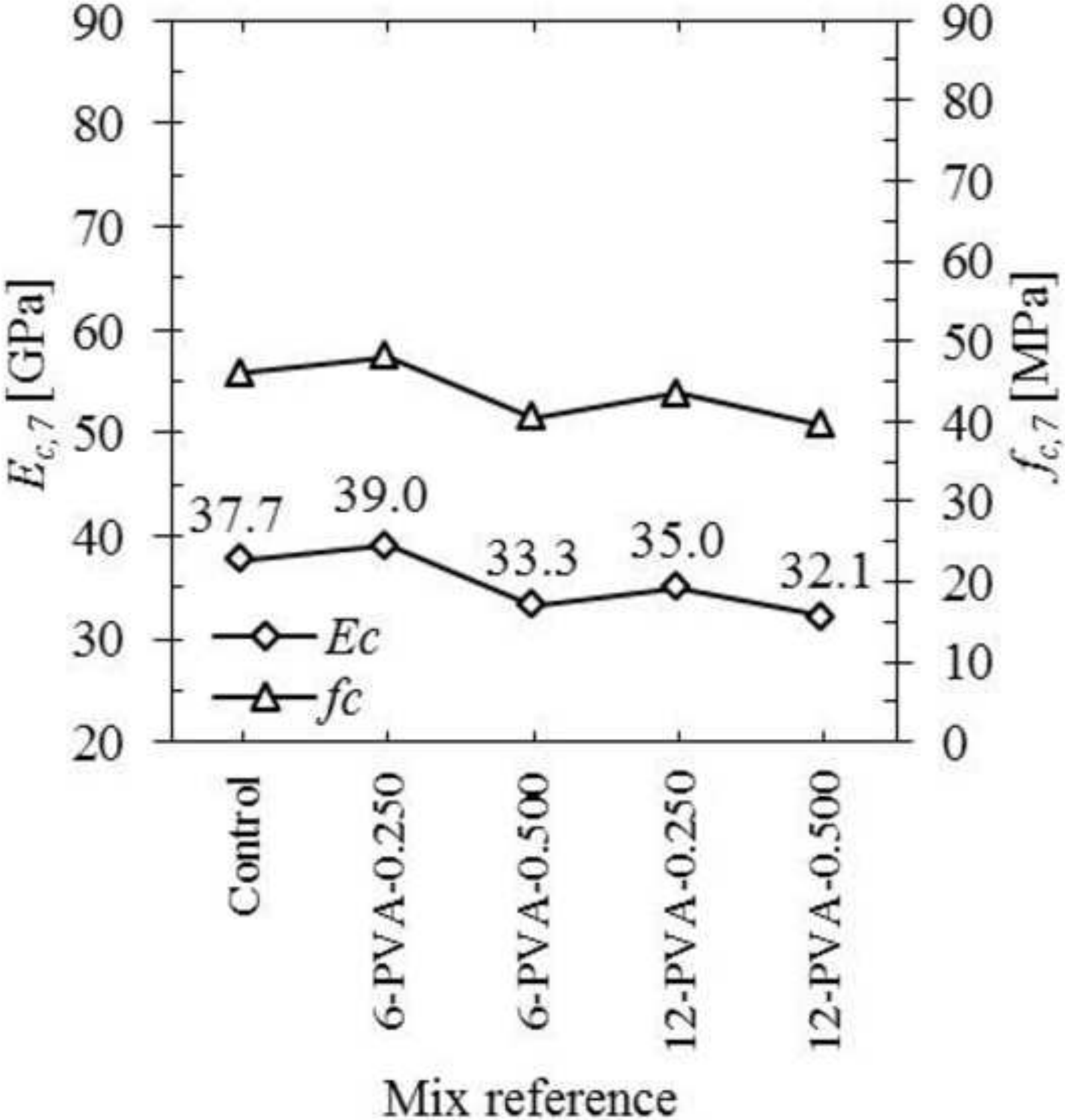

Figure 16b
Click here to download high resolution image

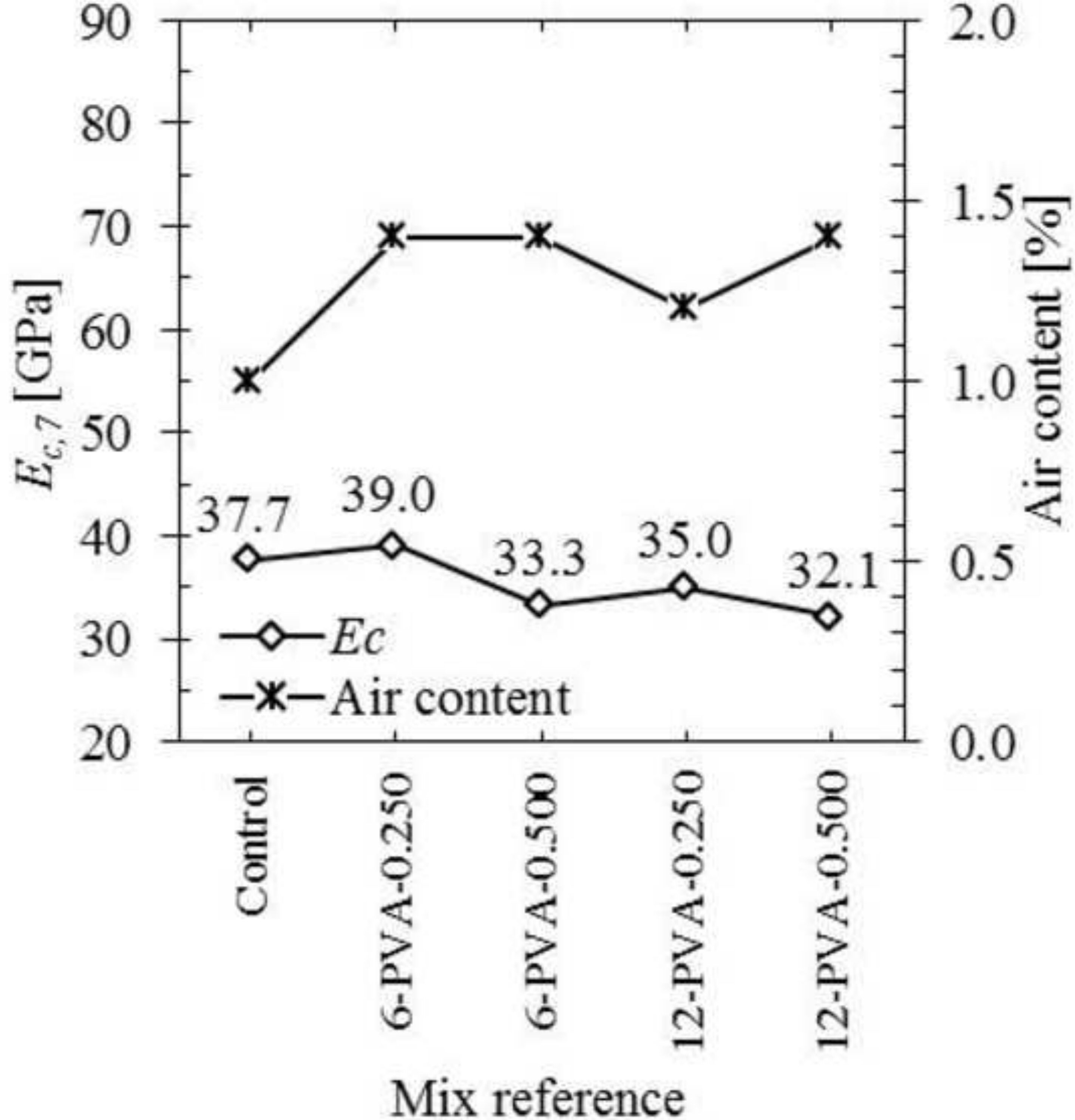

Figure 17a
Click here to download high resolution image

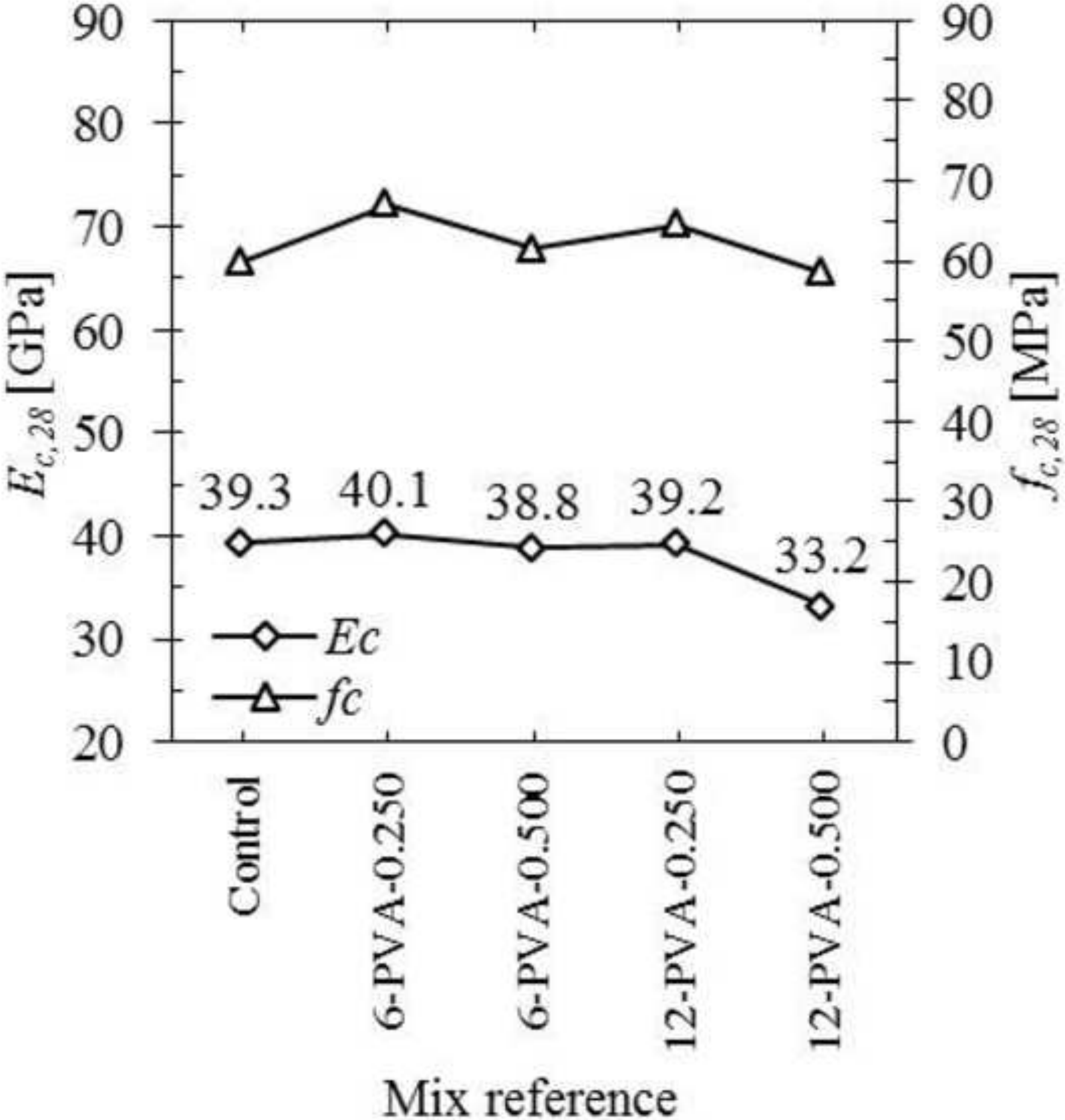

Figure 17b
Click here to download high resolution image

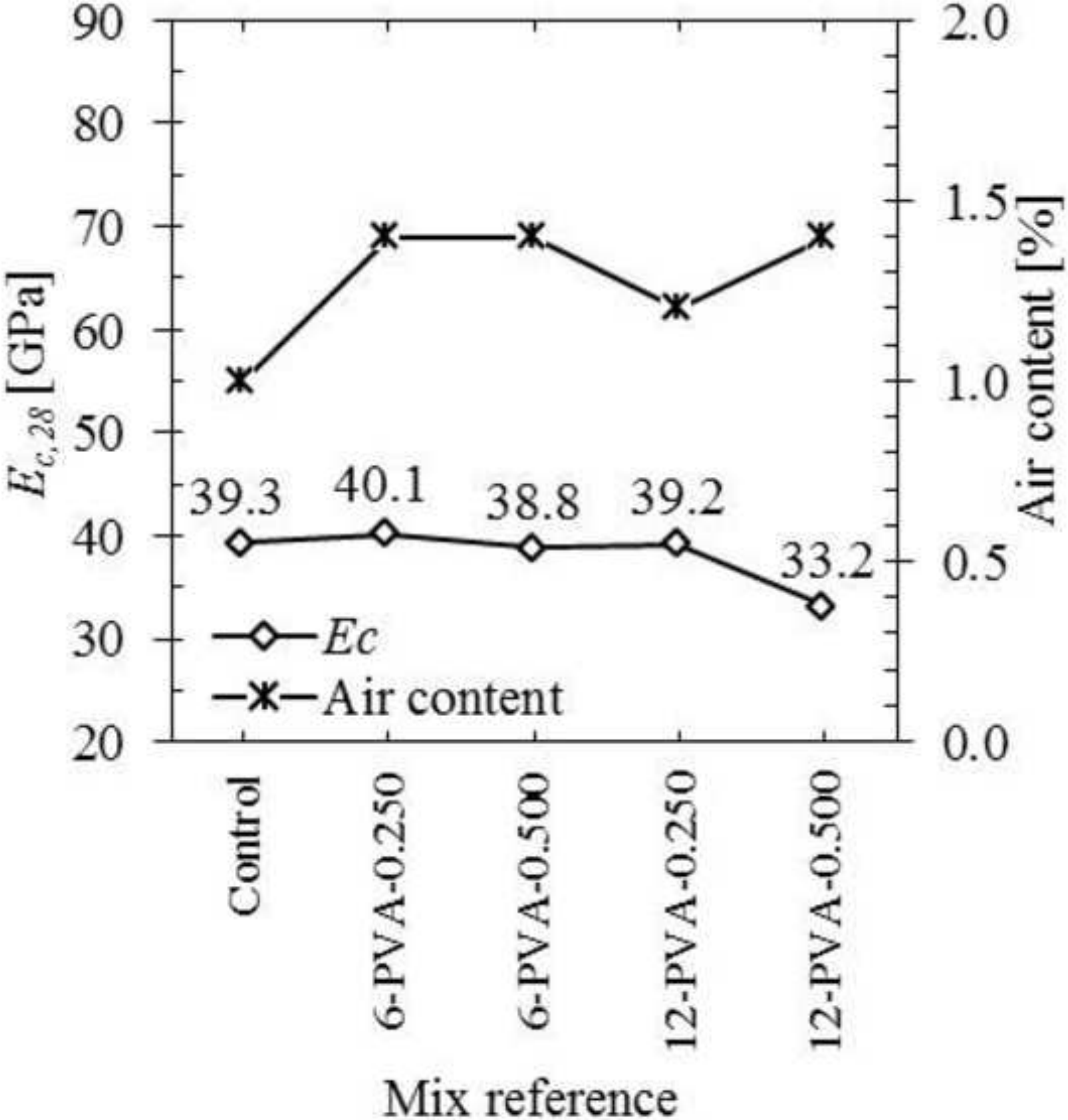

Figure 18a
Click here to download high resolution image

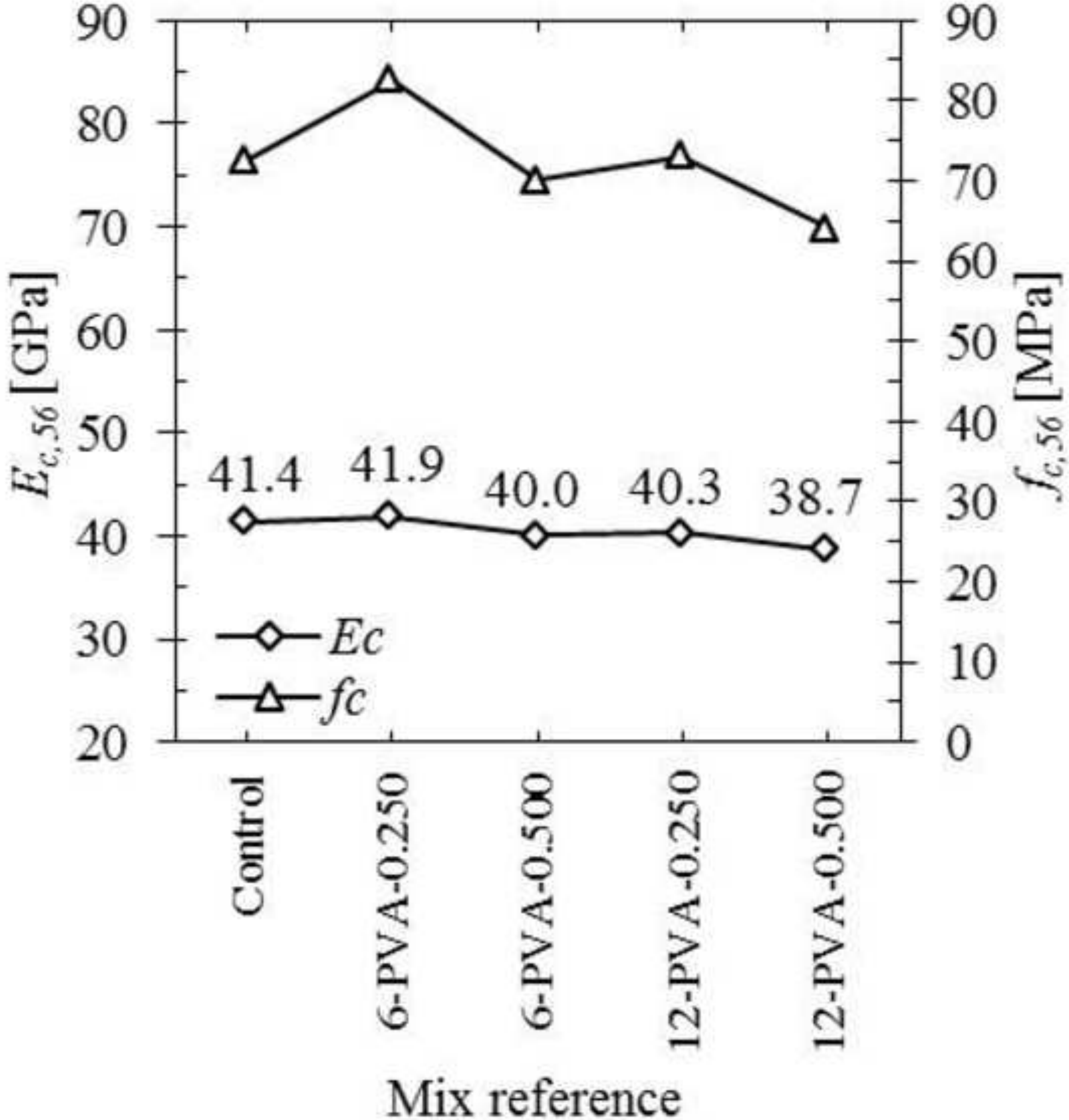

Figure 18b
Click here to download high resolution image

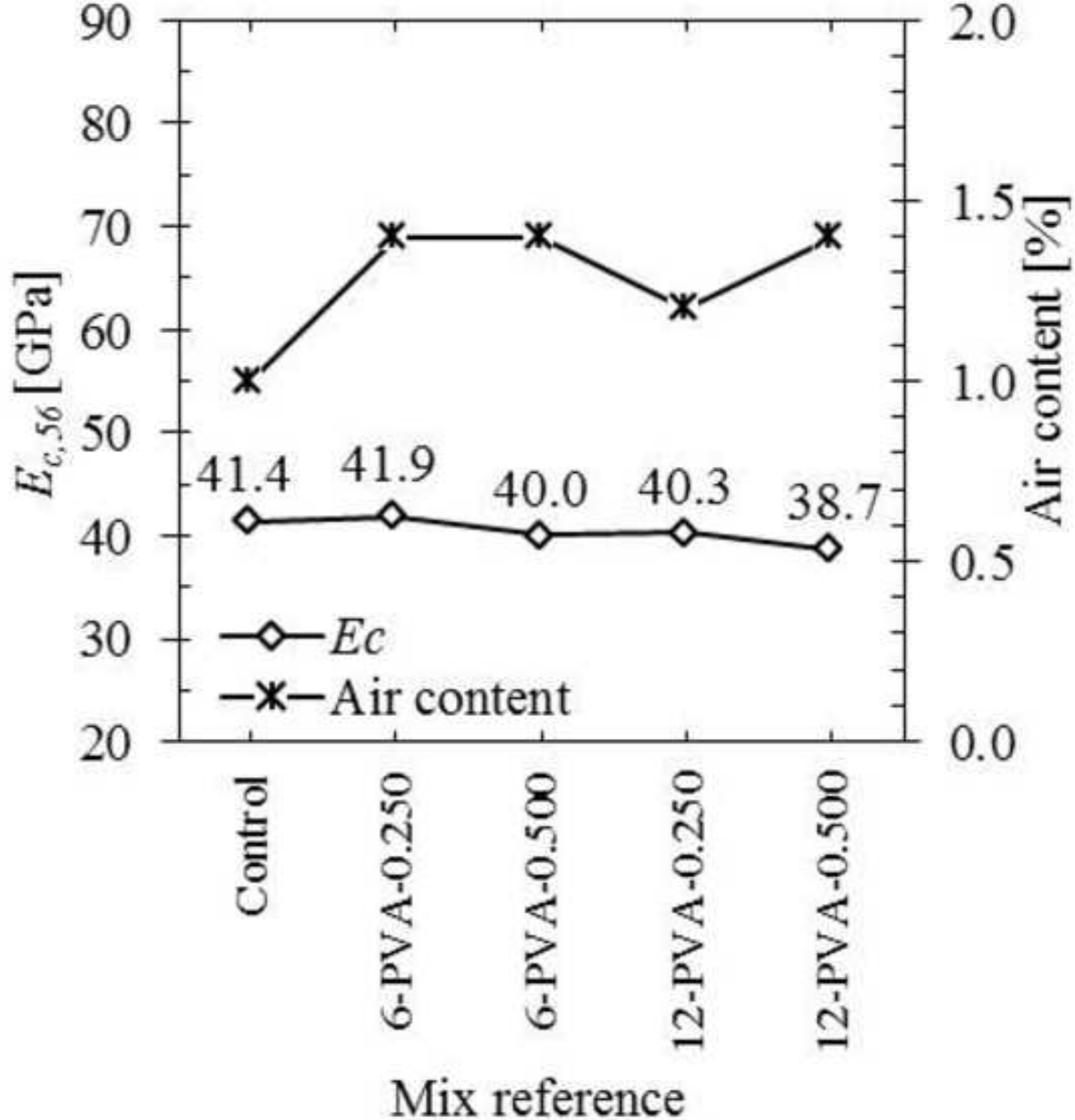

Figure 19

Click here to download high resolution image

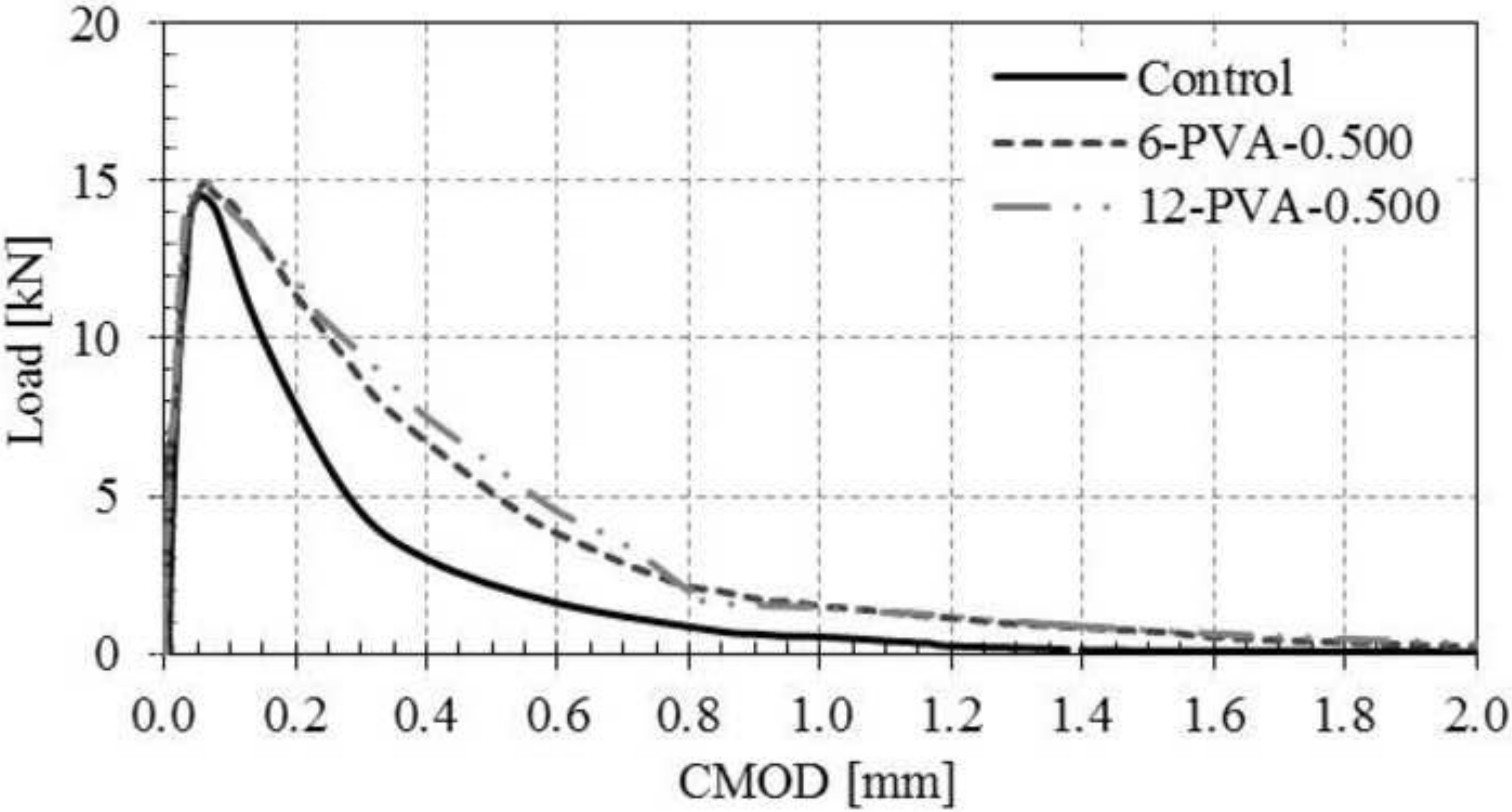

Figure 20

Click here to download high resolution image